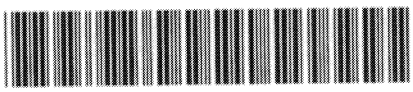

MICHIGAN STATE UNIVERSITY

National Superconducting Cyclotron Laboratory

REACHING THE LIMITS OF NUCLEAR STABILITY

Review article for Rep. Prog. Phys.

M. THOENNESSEN

MSUCL-1285 **JUNE 2004**

REVIEW ARTICLE

Reaching the limits of nuclear stability

M. Thoennessen

National Superconducting Cyclotron Laboratory and
Department of Physics & Astronomy
Michigan State University, East Lansing, MI 48864, USA

E-mail: thoennessen@nscl.msu.edu

Abstract. The limits of nuclear stability have not been reached for most elements. Only for the lightest elements are the minimum and maximum number of neutrons necessary to form an isotope for a given element known. The current limits, novel features of nuclei at these limits as well as the future possibilities of pushing these limits even further will be discussed.

Submitted to: *Rep. Prog. Phys.*

Contents

1. Introduction

Reaching limits has always been a major driving force for explorations in every field of science. In addition to the pure curiosity of finding something new, something that nobody else has ever observed before, the observation (or non-observation) of new type of matter or the discovery of new particles yields crucial information for the understanding of the underlying forces.

Nuclei, consisting of a combination of protons and neutrons, can be pushed to many limits. These limits are typically reached by the collision of two nuclei. At moderate beam energies ($\sim$ 10 MeV/nucleon), the two nuclei can fuse into a compound system which due to the collision starts rotating. Very fast rotating nuclei can change their shape to be extremely deformed before they ultimately reach the fission limit [1, 2]. At higher energies the compound system reaches a temperature limit where it will disintegrate by multifragmentation [3]. The collision of two heavy nuclei at even higher energies leads to densities and temperatures at which the protons and neutrons of the nucleus seize to exist as individual identifiable entities. A new form of matter, a plasma consisting of quarks and gluons may be formed [4, 5, 6].

The limit discussed in this review concerns the question: which combinations of neutrons and protons can form a nucleus? The number of protons (Z) in a nucleus determines the element, and the quest for the heaviest element continues to be an exciting field of research. This is a topic in itself and has been reviewed on a continuous basis as the limit has been pushed to heavier and heavier elements [7, 8, 9]. Just as interesting is the question of what is the largest or smallest number of neutrons (N) that can form a nucleus for any given Z. These limits are called the neutron- and proton-driplines, respectively [10, 11], although the exact definition of the driplines is ambiguous and will be discussed in this review.

Pushing the boundary of knowledge further towards more proton-rich and neutron-rich nuclei has been a priority of nuclear physics for the last 40 years. Exploring the properties of all these nuclei is important for the understanding of the nuclear force, nuclear astrophysics and the formation of the elements. Significant progress has been made since the last major reviews of exotic nuclei and the driplines [12, 10, 13]. A most recent review concentrated on the features of light neutron rich nuclei at and beyond the neutron dripline [11].

The following section will give an overview of the chart of nuclei and the definition of the driplines and nuclei themselves. In section 3 different methods of reaching the driplines will be discussed. The nuclei at and even beyond these driplines can exhibit unusual properties. In particular, these nuclei can potentially exhibit exotic decay modes, for example, neutron radioactivity or di-proton decay. These topics will be discussed in sections 4 and 5 for the proton and neutron dripline, respectively. The astrophysical implications of the location of the driplines will be explored in section 6. Finally new opportunities to reaching and exploring the dripline towards heavier nuclei will be presented in section 7.

2. Nuclear Landscape

There are many combinations of neutrons and protons that can make up a nucleus of a given mass. In the "Table of Isotopes" known properties of all nuclei are published. Since the first publication in 1940 [14] it has grown to several thousands of pages over the last 60 years [15, 16, 17]. It has been customary to use the word isotope

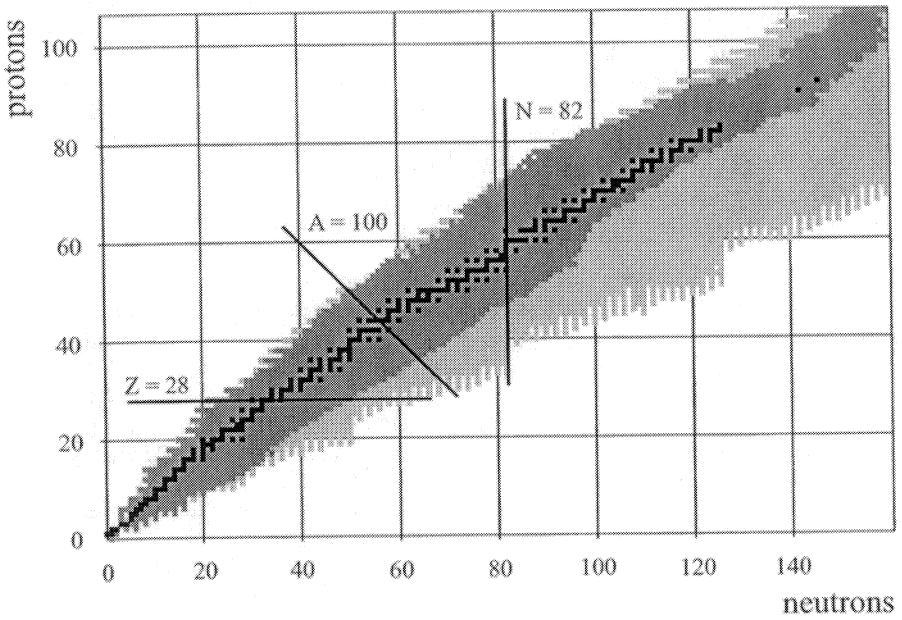

Figure 1. Chart of nuclei: stable (black), presently observed (dark-grey) and still unknown nuclei as predicted by Tachibana *et al.* [18] (light-grey) are shown. The $Z = 28$ isotopes, $N = 82$ isotones and $A = 100$ isobars are indicated by the horizontal, vertical and diagonal line, respectively.

synonymously with nucleus. Strictly speaking, isotopes are defined as nuclei with the same number of protons (Z = constant) but different number of neutrons. Similarly, isotones are nuclei with the same number of neutrons (N = constant) but different number of protons. In addition isobars are nuclei with the same number of nucleons (A = constant).

The chart of nuclei shown in Figure 1 displays the nuclei as a function of neutron number and proton number. A horizontal line corresponds to isotopes, vertical lines to isotones, and diagonals from the top left to bottom right are isobars. The $Z = 28$ isotopes, $N = 82$ isotones, and $A = 100$ isobars are indicated by the horizontal, vertical and diagonal lines, respectively.

There are almost 300 stable nuclei (with a lifetime greater than 10^9 years) which are indicated by the black squares in Figure 1. All other nuclei convert to these nuclei via radioactive decay with different lifetimes that span from nanoseconds to millions of years. For masses up to $A = 209$ typically one or two stable isobars exist for each mass. A few exceptions are for example $A = 5$ and 8 for which there are no stable isobars and $A = 96$ which has three stable isobars (^{96}Ru, ^{96}Mo, ^{96}Zr). Over 2500 of these nuclei are known and shown in dark-grey in the figure. However, there could be as many as an additional 5000 nuclei that have yet to be discovered. Potentially bound nuclei as predicted by Tachibana *et al.* [18] are shown in light-grey.

Isobars with the lowest mass are stable where the mass is given by (see also top

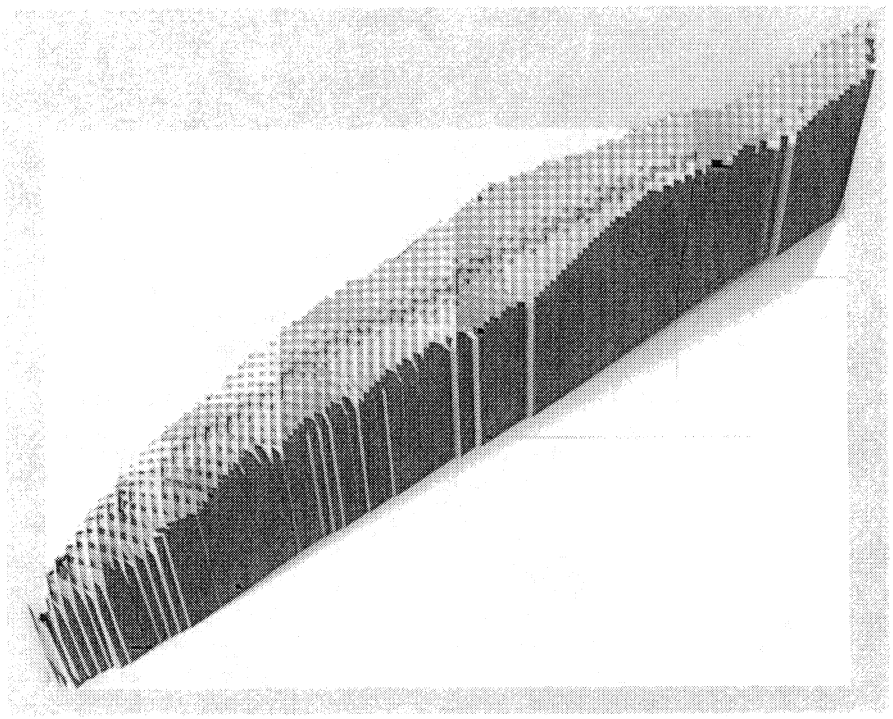

Figure 2. Binding energy per nucleon (E_B/A) as a function of N (x-axis) and Z (y-axis). The darker squares indicate stable nuclei.

part of figure 4):

$$M = Z * m_H + N * m_n - E_B/c^2 \tag{1}$$

with $m_H = 938.8$ MeV/c^2 and $m_n = 939.6$ MeV/c^2. E_B corresponds to the binding energy which is unique for each nucleus. Changing protons into neutrons or neutrons into protons increases the mass (or energy: $E = Mc^2$) of the stable isobars and reduces the binding energy. The binding energy per nucleon (E_B/A) corresponds to the average binding energy for a nucleon within the nucleus. Figure 2 shows E_B/A as a function of Z and N in a surface plot. The figure reveals some of the nuclear structure features. The odd-even staggering shows the increased binding energy due to pairing of two neutrons or two protons. Additional binding occurs also for nuclei with magic numbers of protons and neutrons which occur when major shells are filled. The lines for the magic numbers of 8, 20, 50, 82 and 126 are indicated in the figure and show up as slight ridges in the surface plot. The most bound nuclei in terms of E_B/A are ^{64}Ni and ^{58}Fe. Overall the binding energy per nuclei stays fairly constant around 8 MeV with only a small reduction towards the edge of stability and towards the upper and lower ends of the nuclear chart.

The binding energy per nucleon represents the overall binding of nuclei, however, the question of stability in terms of neutron and proton numbers is not determined by this average quantity, but by the energy necessary to bind the last or least bound

nucleon. This separation energy corresponds to the energy required to remove a single nucleon from a nucleus. The neutron separation energy S_n and proton separation energy S_p can be calculated from the difference of the binding energies of two corresponding adjacent nuclei:

$$S_n = E_B(Z,N) - E_B(Z,N-1) \quad (2)$$

$$S_p = E_B(Z,N) - E_B(Z-1,N) \quad (3)$$

Figure 3 demonstrates the valley of stability by plotting the separation energies with the larger values towards the negative vertical axis. The figure shows the smaller value of S_n and S_p for a given nucleus. In order to avoid the odd-even staggering only odd-odd nuclei, i.e. nuclei with odd numbers of protons and odd numbers of neutrons, are plotted. The special role of the magic numbers at the shell closures can be seen with the major shells indicated by the darker lines. In addition, the dashed diagonal line shows nuclei with equal numbers of protons and neutrons ($N = Z$ nuclei). The trend of the valley of stability towards more neutron-rich nuclei due to the increasing Coulomb repulsion for heavier nuclei becomes apparent. The figure also shows that the slope for proton rich nuclei is steeper than the slope on the neutron rich side.

2.1. Definition of the Dripline

There is no clear definition of the dripline. In their 1993 review Mueller and Sherrill [10] defined the driplines "... where the last nucleon is no longer bound for the lightest or heaviest isotope and the nucleus decays on the time scale of the strong interactions (10^{-22} s or faster)." The latest edition of the chart of nuclei defined the dripline as: "The value of Z and N for which the last nucleon is no longer bound and for which the nucleus decays on the timescale of 10^{-22}s or faster defines the dripline" [19]. In his recent review, B. Jonson states: "The driplines are the limits of the nuclear landscape, where additional protons or neutrons can no longer be kept in the nucleus – they literally drip out." [11].

In contrast, most theoretical papers use a different definition. B. A. Brown defined the proton dripline as "the boundary beyond which nuclei are unbound to direct proton decay" [20]. This definition was also adopted in the review by Hansen and Tostevin: "(the dripline is) where the nucleon separation energy goes to zero" [21]. Hansen and Tostevin also point out that the dripline should follow the isotones for neutron rich nuclei and the isotopes for the proton rich nuclei. In other words ^{11}Be and ^{14}Be are both dripline nuclei. With the above definition there are no cases for which the dripline is double valued.

For the present review the latter approach is followed and the dripline is defined as the limits where S_n or S_p cross zero. Figure 4 shows the mass (top) and the single proton and neutron separation energies (bottom) for the $A = 21$ isotones as an example. Again, the figure displays positive separation energies towards the negative vertical axis. Nuclei close to the valley of stability decay by converting a proton into a neutron or vice versa and the emission of a β^+ or β^-, respectively. If the difference between neutrons and protons becomes too large, the separation energies can become negative and the last neutron or proton is not bound to the nucleus anymore. These are the nuclei beyond the dripline and they can decay by the emission of a proton or a neutron. They are sometimes also called particle unbound or just unbound nuclei. In the figure, ^{21}C and ^{21}Al are neutron and proton unbound, respectively.

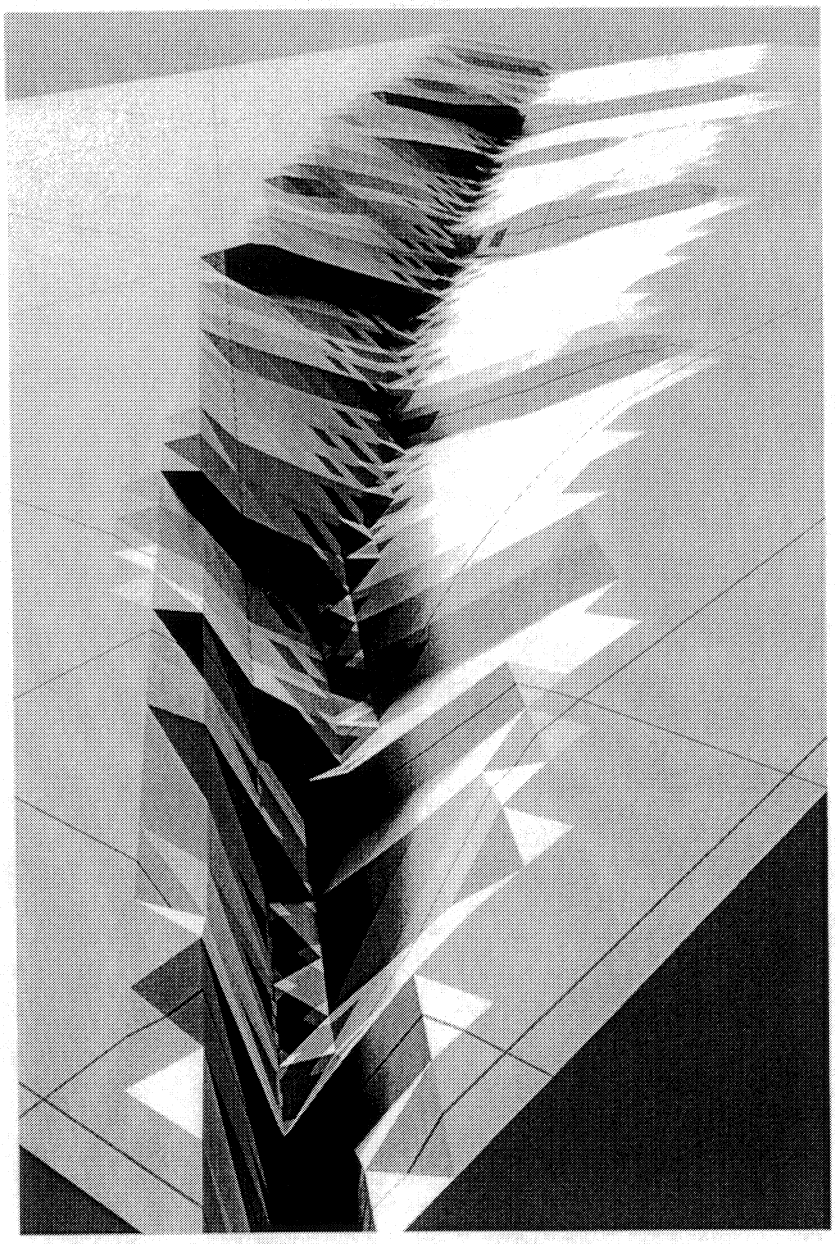

Figure 3. Separation energies as a function of Z (increasing towards the upper left) and N (increasing towards the upper right). For each odd-odd nucleus the numerical smaller value of S_n and S_p is shown with the larger separation energies towards the negative vertical axis. The solid lines indicate the proton and neutron magic numbers and dashed line corresponds to N = Z.

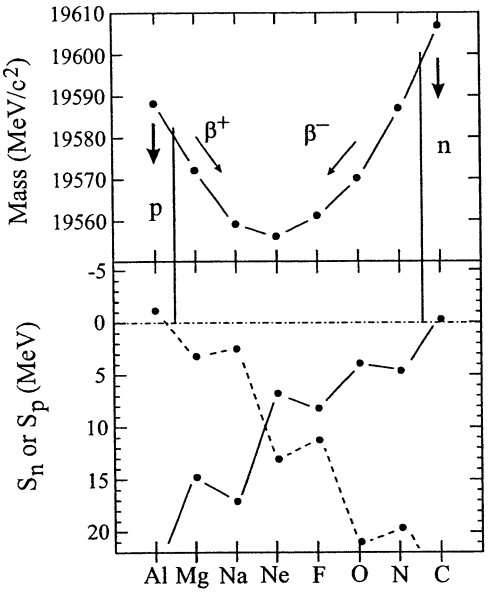

Figure 4. Masses (top) and proton (dashed line) and neutron (solid line) separation energies (bottom) for $A = 21$ isotones from $^{21}Al_8$ to $^{21}C_{15}$.

The decay of an unbound nucleus by the emission of a proton or neutron is sometimes called proton or neutron decay. This terminology can be confused with the decay of the proton or neutron itself. On the other hand, α-decay refers also to the decay of a nucleus by the emission of an α particle and not the decay of the α particle itself.

The separation energy for unbound nuclei is by definition negative and the absolute value of the separation energy corresponds to the energy of the decay: $E_{decay} = |S_{n,p}|$.

2.2. Definition of a Nucleus

The definition of the driplines as the limit where S_n or S_p cross zero determines the location of the dripline unambiguously. However, the definition of the existence of nuclei as an entity is not as clear. Sometimes very short-lived unbound nuclei are not referred to as nuclei at all, but rather only as resonances.

The above definition of the dripline does not limit the existence of a nucleus. Especially at the proton dripline, the emission of a proton from the unbound nucleus can be significantly hindered by the presence of the Coulomb barrier. The unbound proton has to tunnel through the barrier which can lead to significant lifetimes for the emission of the proton. These lifetimes can be even longer than the β^+ lifetimes and even though a nucleus is unbound with respect to proton emission it decays by the emission of a β^+ towards the valley of stability.

In addition to the Coulomb barrier the angular momentum can provide another barrier. For neutron unbound nuclei it is the only barrier that hinders the neutron

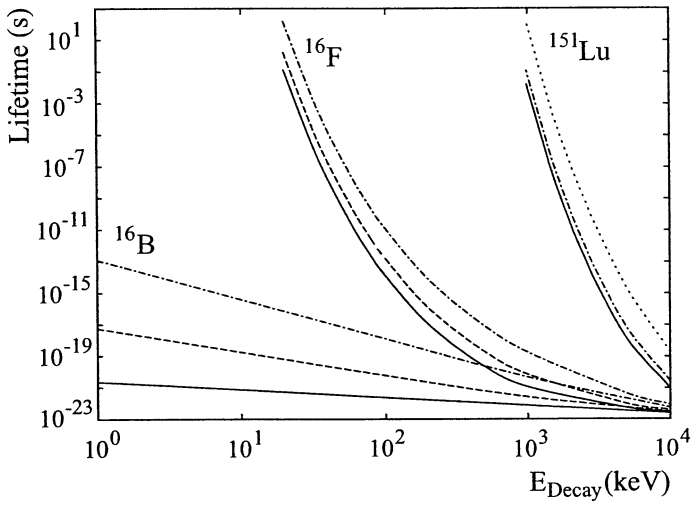

Figure 5. Calculated lifetimes of ^{16}B, ^{16}F and ^{151}Lu as a function of decay energy for angular momenta of L = 0 (——), L = 1 (- - - -), L = 2 (— · —) and L = 5 (· · · · · ·). ^{16}B is a neutron emitter and ^{16}F and ^{151}Lu are proton emitters.

emission.

The influence of the barriers on the lifetime is demonstrated in Figure 5 for neutron and proton emitters with different angular momenta. The possible lifetimes for the neutron unbound nucleus ^{16}B are extremely short and there is only a very small energy range (a few keV) where the decay can have directly measurable lifetimes. On the proton-rich side the lifetimes depend strongly on the charge of the nucleus. While for ^{16}F ($Z = 9$) only decay energies of $\leq$ 100 keV lead to longer lifetimes, energies of 1 to 2 MeV are sufficient for ^{151}Lu ($Z = 71$). The lifetimes also depend strongly on the angular momentum and measured lifetimes have been used to extract the angular momentum state of the emitted nucleon [13].

A potential definition for the existence of a nucleus could be set by the definition of radioactivity. Goldanskii stated that "10^{-12}s corresponds to an approximate limit for radioactivity as such" [22]. This statement was supported later by Cerny and Hardy: "...lifetimes longer than 10^{-12} s, a possible lower limit for the process to be called radioactivity" [23].

This definition would be more restrictive than the definition of an element and thus is inappropriate. The International Union of Pure and Applied Chemistry (IUPAC) has published guidelines for the discovery of a chemical element [24]. In addition to other criteria they state that "the Discovery of a chemical element is the experimental demonstration, beyond reasonable doubt, of the existence of a nuclide with an atomic number Z not identified before, existing for at least 10^{-14}s." The justification for this limit is also given: "This lifetime is chosen as a reasonable estimate of the time it takes a nucleus to acquire its outer electrons. It is not considered self-evident that talking about an 'element' makes sense if no outer electrons, bearers of the chemical properties, are present."

Similarly the definition of a nucleus should be related to the typical time scales

of nuclear motion. Nuclear rotation and vibration times are of the order of 10^{-22}s which can be considered a characteristic nuclear time scale [22]. The above mentioned definitions of the driplines by Mueller and Sherrill [10] and the Chart of Nuclei [19] can be used as the definition of the existence of a nucleus. If a nucleus lives long compared to 10^{-22}s it should be considered a nucleus. Unfortunately this is no sharp clear limit. The most recent editions of the chart of nuclei include unbound nuclei with lifetimes that are on the order of 10^{-22}s [19, 25].

2.3. Experimental Observation of the Driplines

The fact that nuclei exist even beyond the dripline makes the experimental determination of the actual dripline much more complicated. The production and unique identification of a specific nucleus in a reaction is sufficient to claim its existence. Typical direct measurements can identify nuclei with lifetimes longer than $\sim 10^{-9}$s. For shorter lifetimes it is possible to use the uncertainty principle relating the lifetime to the decay width $\Gamma = \hbar/\tau$. Typical detector resolutions in these experiments of the order of keV, however, limit this method to times shorter than $\sim 10^{-19}$s. Thus there is a wide range of lifetimes that is currently not accessible (10^{-10}s -10^{-19}s).

The distinction between dripline and existence is not an issue at the neutron dripline. The shortest β-decay lifetimes are of the order of milliseconds which is well in the range of directly observable nuclei. As shown in figure 5 neutron emission lifetimes are generally much shorter than picoseconds. The observation of direct neutron emission with a lifetime longer than picoseconds would qualify as neutron radioactivity and is an extremely unlikely process because the window of separation energy is extremely small.

Thus the neutron dripline can experimentally be determined as the boundary between directly observed and non-observed nuclei. The difficulty is to decide if the experimental evidence is sufficient to claim the observation of a nucleus or to set an upper detection limit. There have been several cases where claims of existence as well as non-existence have been made based on limited statistics which turned out to be incorrect.

Already in the early 1960's there were controversies about the existence of certain nuclei. ^{5}H was first observed to be particle bound [26], but the existence could not be confirmed in later experiments [27]. First evidence for the observation of ^{21}C and ^{25}O [28] were premature, and these nuclei are unstable with respect to neutron emission and thus beyond the neutron dripline [29]. In contrast ^{14}Be [30] and ^{31}Ne [31], were both first determined to be unbound, but were subsequently observed (^{14}Be [32], ^{31}Ne [33]). Controversial cases at the proton dripline were for example ^{45}Fe [34, 35] and ^{69}Br [36, 37].

The determination of the proton dripline is much harder. The simple observation or non-observation is insufficient to locate the dripline. In order to prove if a nucleus at the proton dripline is bound or unbound, it is necessary to measure the mass of the nucleus with proton and neutron numbers (Z,N) itself, as well as the mass of the nucleus with (Z-1,N). The proton separation energy can then be calculated from the difference of the binding energies (see equations 1 and 3), or directly from the masses:

$$S_p = M(Z-1,N) + M_H - M(Z,N) \tag{4}$$

In order to establish the proton dripline between the nuclei (Z,N) and (Z,N+1) the masses of the four nuclei (Z,N), (Z,N+1), (Z-1,N) and (Z-1,N+1) have to be measured.

In case of the unbound nuclei, it is sufficient to determine a lifetime limit which is shorter than the shorter β-decay lifetimes ($\sim$ 1 ms). Of course, the direct observation of an emitted proton is also sufficient proof that a nucleus is beyond the dripline.

2.4. General Features of the Dripline

The edges of the light-grey area of figure 1 and the edges of the valley shown in figure 3 correspond to the driplines as predicted by the mass model of Tachibana, Uno, Yamada and Yamada [18]. Overall the neutron dripline is significantly further from the valley of stability than the proton dripline.

The horizontal staggering of the proton dripline and the vertical staggering of the neutron dripline is due to pairing. The pairing of two protons or two neutrons adds significant stability to the nucleus so that even-Z nuclei are more stable toward the proton dripline compared to odd-Z nuclei and even-N nuclei are more stable than odd-N nuclei toward the neutron dripline. The staggering is not as obvious in figure 1 for medium mass nuclei ($40 \lesssim Z \lesssim 80$) along the proton dripline because it also displays odd-Z nuclei located beyond the proton dripline which have already been observed.

The influence of shell effects is also apparent in figure 3. For example the $N =$ 50, 82 and 126 isotones are significantly more stable than isotones just above these shell closures. The figure also shows that closed neutron shells shape the landscape for the neutron-rich nuclei but have essentially no effect on the proton-rich side (see for example the $N = 50$ line). The same is also true for the closed proton shells. While the $Z = 20$ shell forms a sharp ridge for proton rich nuclei it has no influence on the neutron-rich side. One of the most interesting current questions is if these traditional shell closures still exist for very neutron (or proton) rich nuclei [38, 39].

Approaching the proton dripline is typically discussed for isotopes (constant Z). Thus the nuclei closer to the dripline should be described as neutron-deficient rather than proton-rich. In order to be consistent, the neutron dripline should then be discussed for isotones (constant N) instead of isotopes [21]. The present practice of describing the neutron dripline in terms of isotopes is problematic due to the odd-even staggering. For example, ^{27}F, ^{29}F, and ^{31}F are bound, while ^{28}F and ^{30}F are unbound. ^{32}F is most likely unbound. However, in order to confirm that the dripline has actually been reached, a definite measurement of ^{33}F is necessary. Changing the description to isotones eliminates this discussion and it is clear that the neutron dripline in this region has been reached for all isotones up to $N = 23$ assuming that ^{30}O is unbound. In the following the neutron dripline will be discussed in terms of isotones.

3. Production of Nuclei at the Dripline

Over the years several different experimental techniques were developed to reach the driplines. Figure 6 shows the first observation of exotic nuclei with $Z \leq 20$ (Calcium) as a function of time.

The black squares correspond to stable nuclei, the light grey squares are nuclei first observed prior to 1960, and nuclei discovered in the subsequent years are shaded as indicated in the figure.

It is obviously easiest to reach the dripline in the lightest nuclei where the driplines are very close to the valley of stability. The proton dripline up to $Z = 11$ (^{20}Na) and the neutron dripline up to $N = 9$ (^{14}B) were already reached by 1966. Single or multiple particle transfer reactions with stable beams and targets as well as target

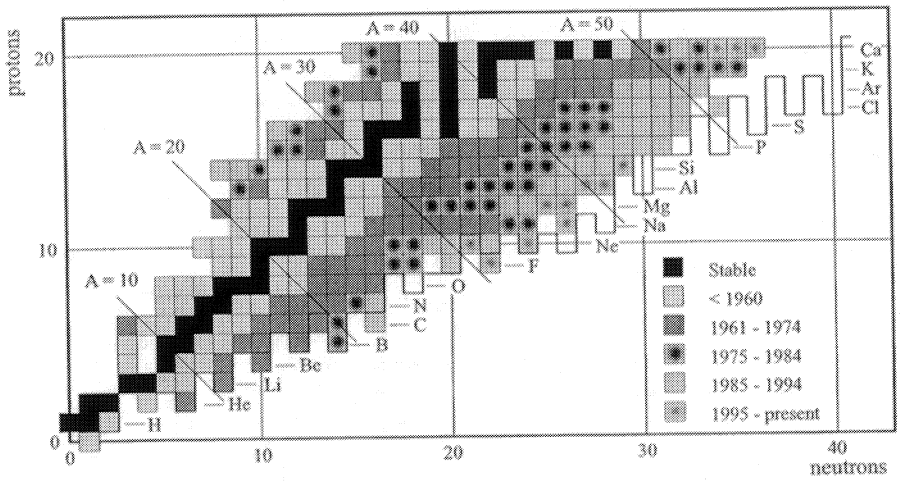

Figure 6. Bound observed nuclei for $Z \leq 20$ (Calcium). The different shadings indicate the time of first observation of the nuclei.

spallation reactions were used to reach the dripline. The increased use of heavy-ion fusion evaporation reactions in the early 70's explored more proton rich nuclei, while in 1971 deep inelastic reactions began to extend the knowledge of neutron-rich nuclei. However, in spite of these developments, by 1974 the proton dripline was only extended by one additional proton ($Z = 12$, ^{20}Mg) and the neutron dripline by three neutrons ($N = 12$, ^{17}B). The exploration of the driplines towards significantly larger proton and neutron numbers was made possible by the development of the projectile fragmentation method in 1979 [40].

Figure 7 shows the different production mechanisms used to observe proton and neutron-rich nuclei for the first time up to $Z \leq 20$. Figure 8 displays only the production of nuclei along the proton dripline up to $Z < 98$. The subsequent discussion will concentrate on these regions because it is unlikely that the proton dripline will be explored beyond $Z = 93$ and the neutron dripline beyond $N = 40$ in the near future.

In the present review the first observation of nuclei is defined by the first publication in a refereed journal. Observations of nuclei reported earlier in annual reports or conference proceedings are not considered.

Again, black squares are stable nuclei, white squares are nuclei discovered before 1960 and the shading of the other nuclei corresponds to the production mechanism of the first observation as indicated in the figure. With the exception of ^{39}Sc only nuclei with lifetimes larger than $\sim 10^{-9}$s are shown corresponding to the location of the driplines in this mass region. In addition to transfer, deep inelastic, target spallation and projectile fragmentation a few nuclei have been first observed with pion exchange reactions and fission of relativistic beams. Projectile fragmentation is the method of choice to reach the neutron dripline for $N < 40$ and also the proton dripline for $Z < 50$. For heavier nuclei fusion evaporation is presently the only competitive method to reach the proton dripline.

In the following discussion, the separation between the different techniques is based on the production mechanism rather than the subsequent separation mechanism.

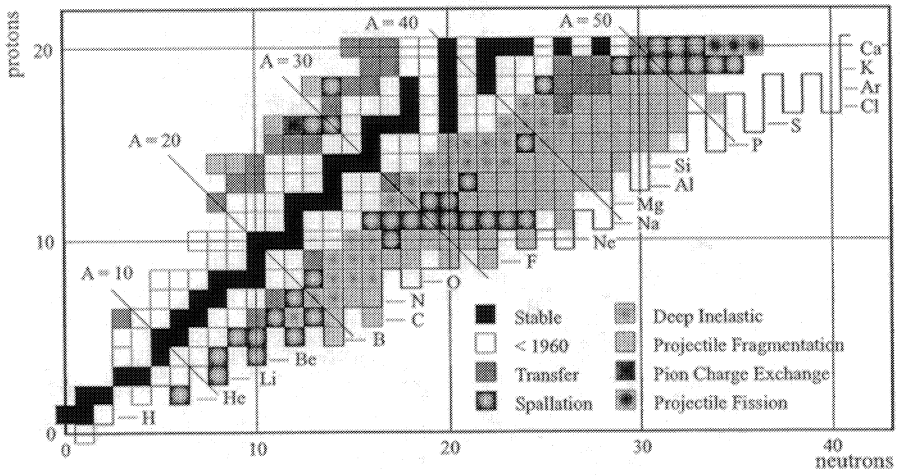

Figure 7. Observed nuclei along the proton and neutron dripline for $Z \leq 20$. The different shadings indicate the experimental detection method of first observation.

This classification is not unique, for example, in addition to target spallation, transfer and fusion evaporation reactions can also be stopped in a thick target and subsequently identified using the ISOL technique (Isotope Separation On Line). On the other hand transfer and fusion evaporation reactions can also occur in thin targets where the recoil energy is sufficient for the reaction products to leave the target which can then be analyzed by recoil mass separators.

In addition, the boundaries between the different production methods are not well defined. For example, the transition from fusion-evaporation to deep inelastic to projectile fragmentation is gradual. Also, even at very high beam energies, projectiles can pickup nucleons from the target, however, in the following this process is also considered projectile fragmentation.

3.1. Transfer Reactions

Transfer reactions are extremely useful to extract detailed structure information. For the exploration of the driplines transfer reactions with stable beams and stable targets are limited to the lightest nuclei. Obviously, simple one- or two-nucleon transfer reactions, for example (p,d), (d,p), (p,t) etc. and single charge exchange reactions like (p,n) and (t,^{3}He) are limited to the study of nuclei close to the valley of stability.

The use of more complicated multiparticle transfer reactions lead to the first observation of the proton dripline nuclei ^{9}C, ^{20}Mg, and ^{22}Al via the reactions ^{12}C(^{3}He,^{6}He)^{9}C [41], ^{24}Mg(α,^{8}He)^{20}Mg [42], and ^{24}Mg(^{3}He,p4n)^{22}Al. Examples for multiparticle transfer reactions populating neutron-rich nuclei are ^{48}Ca(^{6}Li,^{8}B)^{46}Ar [43] and ^{48}Ca(^{3}He,^{8}B)^{43}Cl [44].

Transfer reactions with light ions have also been very successful in studying particle unstable nuclei. For example the reaction ^{7}Li(t,^{3}He)^{7}He was used to prove the instability ^{7}He [45]. At the proton rich side examples for reactions are ^{10}B(^{3}He,^{6}He)^{7}B [46], ^{24}Mg(p,^{6}He)^{19}Na [47] and ^{12}C(α,^{8}He)^{8}C [42].

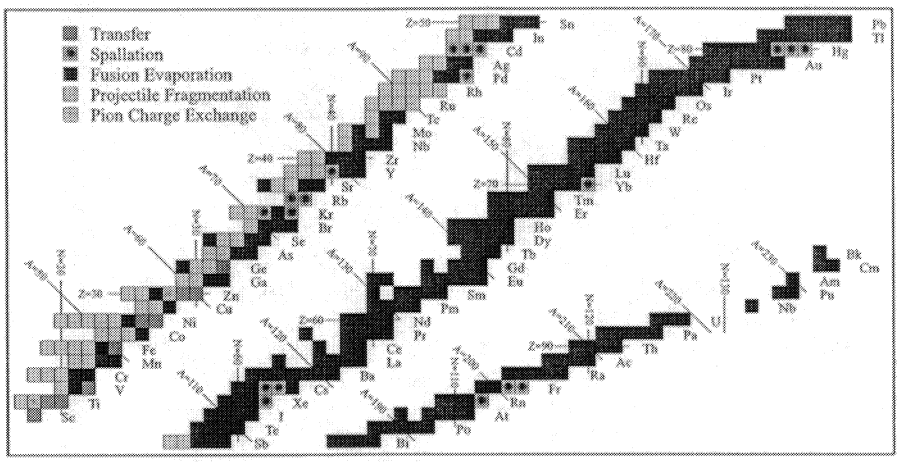

Figure 8. Observed nuclei along the proton dripline for $20 < Z < 98$. The different shadings indicate the experimental detection method of first observation.

The study of unbound nuclei with transfer reactions is always indirect. The unbound nucleus decays instantaneously in the target and thus cannot be analyzed in a magnetic separator. The energy levels of the unbound nucleus however can be inferred from the energy-loss spectrum of the ejectile. It is advantageous if the ejectile itself does not have any bound excited states in order to avoid misidentification of excitations in the unbound nucleus and the ejectile.

3.2. Fusion Evaporation

Fusion evaporation reactions have been very successful in exploring the proton dripline especially above $Z = 50$, where at the present it is essentially the only way to produce nuclei at and beyond the dripline. This technique is limited to the proton dripline because of the curvature of the valley of stability towards neutron-rich nuclei and the preferential evaporation of neutrons during the cooling of the fused compound nuclei.

Nuclei close to the dripline have been populated with fusion evaporation reactions as early as 1964. ^{108}Te and ^{109}Te have been identified by their α decay following the reactions ^{96}Ru(^{16}O,4n)^{108}Te and ^{96}Ru(^{16}O,5n)^{107}Te [48].

Pushing closer to the limit involved smaller and smaller cross sections, thus requiring more sophisticated separation and detection techniques. With the development of velocity filters [49] and mass separators [50] tremendous progress was made along the proton dripline. The experimental techniques are described in detail in the review by Woods and Davids [13].

The accessibility of the proton dripline with fusion evaporation reactions relies on the availability of stable target projectile combinations. Figure 9 is the same as figure 1, with the addition of all compound nuclei that can in principle be produced with fusion evaporation reactions using any combination of all stable beams and targets. These compound nuclei are indicated by the small dots. Assuming that the xn or pxn evaporation channels (with x between 2 and 6) can be separated and identified the figure shows that the dripline can be explored above $Z = 30$. It can be seen in the figure

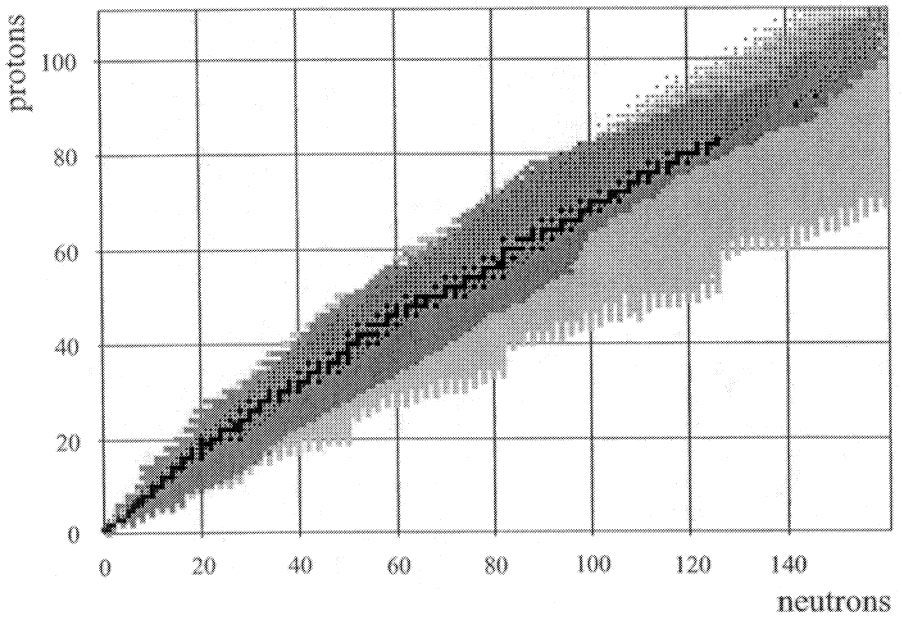

Figure 9. Chart of nuclei: stable (black), presently observed (dark-grey) and still unknown (light-grey) nuclei are shown. The small dots represent compound nuclei that can be populated by fusion reactions with all possible combinations of stable projectiles and stable targets. Dripline nuclei can be reached by multiple neutron evaporation.

that above $Z = 50$ a few specific choices of target and projectile combinations get really close to the dripline, making fusion evaporation an effective tool to reach the dripline in this region (see also tables 3 and 5). Although it seems that the dripline should be reachable beyond $Z = 80$ this is apparently not the case. In order to populate these very proton-rich heavy nuclei very symmetric projectile target combinations have to be chosen. The Coulomb barrier for these reactions are large, so that it is not possible to produce these nuclei at excitation energies where none or only one proton is evaporated. These excited compound nuclei decay by fission or α-emission. In addition, not all target projectile combinations are practical.

3.3. Target Spallation

Target spallation was the first method that reached the dripline for nuclei which were not accessible with simple transfer reactions. Dripline nuclei up to $N = 13$ (^{19}C) were first observed using target spallation.

In 1965 Poskanzer *et al.* [51] bombarded a ^{15}N target with 2.2 GeV protons. They were able to show the existence of ^{12}Be via the (p,4p) reaction. With the development of semiconductor detectors it became possible to identify nuclei directly, without measuring the subsequent decay [52]. The addition of time-of-flight measurements to the particle identification technique with silicon telescopes increased the sensitivity even further. ^{17}C [53] ^{19}N and ^{21}O [54] were first observed with this technique.

Another major step forward was the development of online mass spectrometry. This method was especially competitive for alkali metals which could easily diffuse out of heated graphite targets [55]. In a series of experiments at ISOLDE sodium isotopes from ^{27}Na up to ^{35}Na were observed [55, 56, 57, 58].

Although a very important method to produce rare isotopes, target spallation can compete with fusion evaporation and projectile fragmentation for the exploration of new nuclei along the dripline in only a very few specific cases. More experimental details of target spallation can be found in references [59, 60].

3.4. Deep Inelastic Reactions

Deep inelastic reactions occur typically in a beam energy range between 5 and 10 MeV/nucleon. It refers to reactions where the target and projectile exchange a certain number of nuclei. There is not a clear distinction between deep inelastic reactions and fusion evaporation on one hand and projectile fragmentation on the other. In figures 7 and 8 reactions with energies below 10 MeV/nucleon are considered deep inelastic reactions, while energies above 35 MeV/nucleon are considered projectile fragmentation. The energy regime between these values has not been used to produce new nuclei.

Deep inelastic reactions were first successfully used to explore neutron-rich nuclei from Carbon to Chlorine [61, 62, 63, 64, 65].

3.5. Projectile Fragmentation

Projectile fragmentation, as the next step up in beam energy from deep inelastic reactions, was first used to produce neutron rich nuclei in 1979 [40]. Beginning in 1985 [66] it was also used to explore the proton dripline. Experimental details of this method can be found in references [60, 67].

Just like fusion evaporation the success of projectile fragmentation is based on the extremely high level of sensitivity. In order to identify the most exotic nuclei of interest it is necessary to separate them not only from the intense primary beam, but also from the large number of other fragments that are produced simultaneously.

Figure 10a shows the distribution of fragments following the fragmentation of 140 MeV/nucleon ^{48}Ca on a ^{9}Be target. The initial ^{48}Ca intensity is 10^{12} particles per second. The selection of the isotope of interest is achieved by a magnetic separator located immediately behind the target. Figure 10b shows the isotopes transmitted by the separator tuned in this specific case for ^{31}F which is produced only with an intensity of a few nuclei per hour. If the number of overall events are still too large for the rarest events to be observed an energy-degrading wedge can be inserted in the center of the separator and a second stage of magnetic separation can reduce the number of unwanted fragments even further as seen in figure 10c. The rates of figure 10 were calculated with LISE++, a general purpose fragmentation code [68, 69].

Projectile fragmentation is currently the only mechanism to explore new nuclei at and beyond the neutron dripline and it also has been the dominant production mechanism to push the proton dripline below $Z \sim 50$ to its present limit.

For a few special cases projectile fragmentation has also been used to populate and study particle unstable nuclei. The decay of ^{7}He, ^{10}Li and ^{13}Be in flight following the production from a ^{18}O beam was measured by coincidence detection of the emitted neutron and the fragment [70, 71, 72].

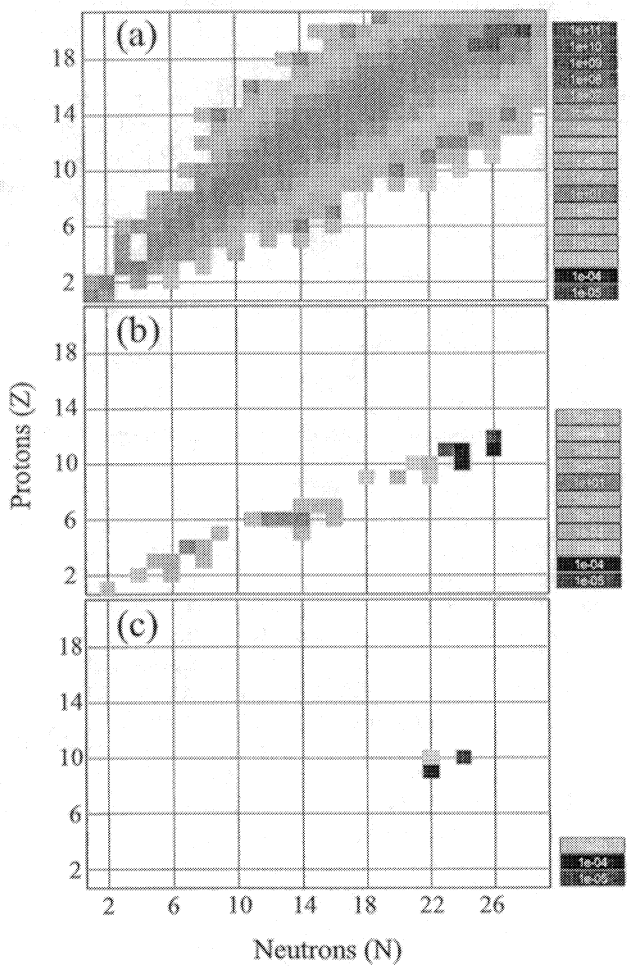

Figure 10. Production of dripline nuclei using fragmentation of ^{48}Ca: (a) intensity distribution of all produced secondary fragments, (b) nuclei selected following magnetic separation, (c) additional purification of ^{31}F using a second stage separation.

3.6. Pion Exchange Reactions

In a few special cases pion double charge exchange reactions were used to observe nuclei for the first time. For example ^{28}S and ^{40}Ti were populated by the reactions ^{28}Si$(\pi^+,\pi^-)^{28}$S and ^{40}C$(\pi^+,\pi^-)^{40}$Ti [73].

Similar to transfer reactions, pion charge exchange reactions can also be used to study unbound nuclei, because the energy levels of the product nucleus is deduced from the energy-loss spectrum of the π^- ejectile. States of unbound ^{9}He [74] and most recently ^{6}H [75] were observed with this technique.

3.7. Fission of Fast Beams

Figure 7 shows that the first observation of the neutron-rich Calcium isotopes $^{54-56}$Ca was achieved by fission of fast beams [76]. In this experiment, a total of 58 new nuclei were produced in projectile fission of 750 MeV/nucleon ^{238}U. The new nuclei ranged from calcium (^{56}Ca) to silver (^{127}Ag) with A/Z ratios of up to 2.8. However, the dripline in this mass region is predicted significantly further away at about ^{70}Ca and ^{155}Ag or A/Z ratios of approximately 3.4.

In the near future, it is not anticipated that even this powerful technique of projectile fission will be able to reach the dripline in this mass region.

3.8. Reactions with Rare Isotopes

With the increasing intensities of rare isotope beams, produced either by the ISOL method or by projectile fragmentation, it has become feasible to use these beams for secondary reactions.

For example elastic and inelastic scattering [77], Coulomb excitation [78, 79], transfer [77, 80, 81], knock-out [21] and most recently secondary fragmentation [82] have been used to study properties of neutron and proton-rich nuclei. Except for the secondary fragmentation, the references refer to reviews of the topics. The intensities of rare isotope beams are presently not sufficient to use these reactions to explore the dripline themselves with the exception of the very lightest elements.

In the lightest mass region, however, reactions with rare isotopes play already an important role in the study of unbound nuclei. For example, resonances in ^{7}H and ^{10}He were first observed with single charge exchange reactions [83, 84]. In addition, single proton knock-out reactions confirmed that ^{16}B [85] and ^{25}O [86] are unbound.

At the proton-rich side, single neutron knock-out reactions populated the unbound nuclei ^{12}O [87], ^{11}N [88] and ^{19}Mg [89]. More complicated transfer reactions populated ^{18}Na and ^{19}Na [89]. In addition, elastic resonance scattering of rare isotopes was used to determine ground- as well as excited states in the unbound nuclei ^{11}N [90, 91], ^{15}F [92] and ^{19}Na [93].

4. Proton Dripline

The proton dripline has been studied since the beginning of nuclear reactions, because it is much closer to the valley of stability than the neutron dripline. For ^{4,5}Li the proton dripline is located right next to the stable isotopes of ^{3,4}He and ^{6}Li. In addition, as shown in figure 9, fusion evaporation reactions always populate proton rich nuclei making the proton dripline more accessible than the neutron dripline. By 1987 all nuclei on the proton rich side expected to be particle stable up to $Z = 23$ (Vanadium) had been observed. Today, the dripline has been reached for all odd Z nuclei up to $Z = 91$. Bound nuclei that have yet to be discovered are limited to even Z nuclei in the regions from $Z = 32$ through $Z = 64$ and for $Z \geq 82$. As mentioned earlier, only nuclei which have been reported in refereed publications are included in the present review.

Although nuclei at and beyond the dripline have been observed for almost all the elements, it is surprising that the actual location of the dripline is known for only a few elements. As was discussed in section 2.3 the experimental determination of the proton dripline involves the measurement of several masses in the vicinity of the dripline. With extrapolations and interpolations from known masses and decay

energies the proton dripline is probably fairly well predicted, but purely experimentally the dripline has only been determined up to $Z = 12$ (magnesium), and then again only for a few elements, for example scandium, lutethium and tantalum.

4.1. Light Mass Nuclei: $Z \leq 20$

The proton dripline was reached up to sodium ($Z = 11$) already by 1960. Table 1 lists the reactions populating the most neutron-deficient isotopes for the heavier elements.

They are most likely the limit of isotopes with lifetimes longer than a millisecond. The significant shorter lifetimes of the unbound isotopes have been determined for ^{7}B [46], ^{8}C [42], ^{10}N [100], ^{11}N [101], ^{12}O, ^{15}F, ^{16}Ne [102], ^{19}Na [47], and ^{18}Na [89]. ^{15}F was reported simultaneously in reference [103].

For ^{19}Mg [104] and ^{21}Al [95] upper limits of the lifetime were measured. Although not explicitly stated in figure 3 of reference [97] it can be concluded that ^{25}P, ^{29,30}Cl and ^{33,34}K are beyond the proton dripline and have lifetimes shorter than the time-of-flight of 170 ns. However, this is not true for the even-Z nuclei ^{26}S, ^{30}Ar and ^{34}Ca. As stated in reference [97]: "The steepness of the valley of β stability on the proton-rich side and some remaining background events do preclude any definite statement as to the non-observation of a given isotope." Also, ^{21}Si has not been explored at all.

Figure 11 shows all nuclei close and beyond the proton dripline. The black squares are stable nuclei and the dark grey squares show all bound observed nuclei. The circled light grey squares are unbound nuclei where spectroscopic measurements have been performed. For the light grey squares upper limits on the lifetime have been reported. The thick solid line shows the measured dripline. The dripline is shown as a dashed line for elements where it has been predicted but not explicitly measured.

The proton dripline is well established up to magnesium. The uncertainties for the odd-Z nuclei begin with ^{22}Al and ^{26}P (striped squares). The latest mass evaluation [105] quotes proton separation energies of 17 ± 95 keV and 140 ± 196 keV for these two nuclei, respectively. Thus it is not clear on which side of the dripline these nuclei are located.

The situation for the even-Z nuclei is different. Although ^{22}Si and ^{31}Ar (dashed squares) are predicted to be bound with respect to one-proton emission, the two proton separation energies, defined as

$$S_{2p} = M(Z-2, N) + 2M_H - M(Z, N) \tag{5}$$

Table 1. Lightest presently observed bound isotopes for $12 \leq Z \leq 20$. The production reaction, laboratory and reference of the first observation are listed.

Z	Isotope	Method	Laboratory	Reference
12	^{20}Mg	^{24}Mg(^{4}He,^{8}He)	Jülich	[42]
13	^{22}Al	^{24}Mg(^{3}He,p4n)	LBL	[94]
14	^{22}Si	Ni(^{36}Ar,X) 85MeV/u	GANIL	[95]
15	^{26}P	^{28}Si(^{3}He,p4n)	LBL	[96]
16	^{27}S	Ni(^{40}Ca,X) 77.4 MeV/u	GANIL	[97]
17	^{31}Cl	^{36}Ar(^{3}He,^{8}Li)	MSU	[98]
18	^{31}Ar	Ni(^{40}Ca,X) 77.4 MeV/u	GANIL	[97]
19	^{35}K	^{40}Ca(^{3}He,^{8}Li)	MSU	[99]
20	^{35}Ca	^{40}Ca(^{3}He,α4n)	LBL	[66]

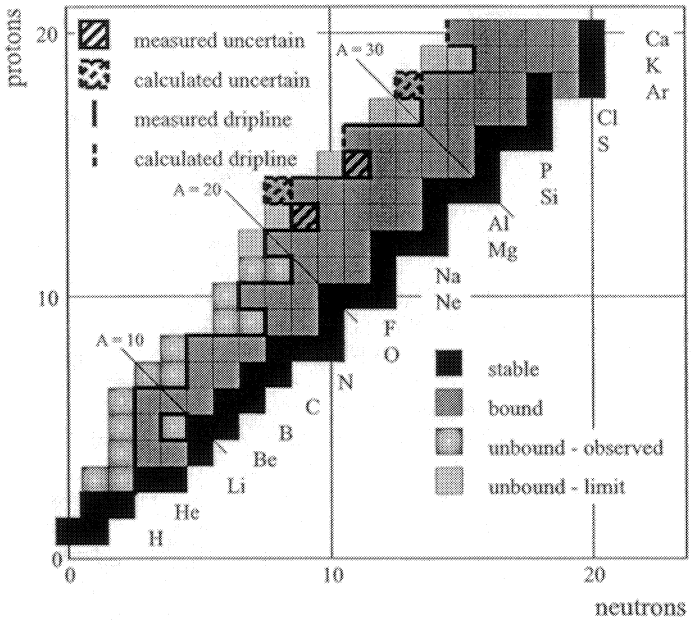

Figure 11. Nuclei at and beyond the proton dripline for $Z \leq 20$.

are calculated to be -16 ± 202 keV (^{22}Si) and 126 ± 212 keV (^{31}Ar). Thus they are possible candidates for di-proton decay. This exotic decay has been predicted already in 1960 [22] and attempts to observe it have been performed in many different systems [13] (see also section 4.6). In the case of ^{22}Si and ^{31}Ar the searches were unsuccessful because, even if these nuclei are unbound with respect to two-proton emission, the decay energy is too small, and thus the lifetimes too long to be able to compete with β-decay.

It should be mentioned that the search for the di-proton decay in this mass region below $Z \leq 12$ has concentrated on larger decay energies. These decays then do not compete with β-decay but the corresponding lifetimes are so short that they cannot be measured with direct techniques. First evidence for the possible observation of di-proton emission has been reported in this mass region for the decay of an excited state of ^{18}Ne [106].

The proton dripline exhibits also changes in the shell structures which is a strong effect at the neutron dripline. The $Z = 8$ closed shell disappears for very proton rich nuclei. The last proton of ^{11}N is not populating the $1p$ state as expected in the normal shell model, but rather the $2s$ state. This level inversion has first been observed in the mirror nucleus ^{11}Be (see section 5.1). The existence of ^{22}Si is due to the emergence of the new shell at $Z = 14$ for nuclei located far away from the valley of stabillity. These effects are less pronounced at the proton dripline relative to the neutron dripline because the proton dripline occurs closer to the valley of stability.

4.2. Medium Mass Nuclei I: $20 < Z \leq 50$

Initially the proton dripline in this mass region was approached with fusion evaporation reactions starting in the early seventies, however, the available stable target projectile combinations are not ideally suited to reach the dripline (see figure 9). With a few exceptions the nuclei at and beyond the dripline were produced with projectile fragmentation. Table 2 lists the most neutron deficient isotopes presently observed.

In this mass region nuclei beyond the dripline begin to have significant lifetimes to survive fragment separator flight times. The Coulomb barrier for proton emission becomes sufficiently large, so that for nuclei with small decay energies β-decay can compete with proton emission. If the nuclei decay by proton emission the lifetimes can be long enough to qualify as proton radioactivity (see discussion in section 2.2). Up to now no proton emitter has been observed in this mass region. However, most recently evidence for two-proton radioactivity was reported in the decay of ^{45}Fe [124, 125] (see also section 4.6).

Figure 12 shows the nuclei along the proton dripline for nuclei with $20 < Z \leq 50$. The notations in the figure are different from figure 11. The valley of stability is not shown. The dark grey squares are nuclei which have been observed with lifetimes longer than approximately 1 μs [126].

Table 2. Lightest presently observed isotopes for $20 < Z \leq 50$. The production reaction, laboratory and reference of the first observation are listed.

Z	Isotope	Method	Laboratory	Reference
21	^{39}Sc	^{40}Ca(^{7}Li,^{8}He)	MSU	[107]
22	^{39}Ti	Ni(^{58}Ni,X) 65MeV/u	GANIL	[108]
23	^{43}V	Ni(^{58}Ni,X) 55MeV/u	GANIL	[109]
24	^{42}Cr	Be(^{58}Ni,X) 600MeV/u	GSI	[35]
25	^{46}Mn	Ni(^{58}Ni,X) 55MeV/u	GANIL	[109]
26	^{45}Fe	Be(^{58}Ni,X) 600MeV/u	GSI	[35]
27	^{50}Co	Ni(^{58}Ni,X) 55MeV/u	GANIL	[109]
28	^{48}Ni	Ni(^{58}Ni,X) 74.5MeV/u	GSI	[110]
29	^{55}Cu	Ni(^{58}Ni,X) 55MeV/u	GANIL	[109]
30	^{55}Zn	Ni(^{58}Ni,X) 74.5MeV/u	GANIL	[111]
31	^{60}Ga	Ni(^{78}Kr,X) 73MeV/u	GANIL	[37]
32	^{61}Ge	^{40}Ca(^{24}Mg,3n)	LBL	[112]
33	^{64}As	Ni(^{78}Kr,X) 73MeV/u	GANIL	[37]
34	^{65}Se	^{40}Ca(^{28}Si,3n)	LBL	[113]
35	^{70}Br	^{58}Ni(^{14}N,2n)	BNL	[114]
36	^{69}Kr	Ni(^{78}Kr,X) 73MeV/u	GANIL	[37]
37	^{74}Rb	Nb(p,4pxn) 600 MeV	CERN	[115]
38	^{73}Sr	^{40}Ca(^{36}Ar,3n)	LBL	[116]
39	^{76}Y	Be(^{112}Sn,X) 1GeV/u	GSI	[117]
40	^{78}Zr	Be(^{112}Sn,X) 1GeV/u	GSI	[117]
41	^{82}Nb	^{58}Ni(^{92}Mo,X) 70MeV/u	MSU	[118]
42	^{83}Mo	Ni(^{92}Mo,X) 60MeV/u	GANIL	[119]
43	^{86}Tc	^{58}Ni(^{92}Mo,X) 70MeV/u	MSU	[118]
44	^{87}Ru	Ni(^{112}Sn,X) 63MeV/u	GANIL	[120]
45	^{89}Rh	Ni(^{112}Sn,X) 63MeV/u	GANIL	[120]
46	^{91}Pd	Ni(^{112}Sn,X) 63MeV/u	GANIL	[120]
47	^{94}Ag	Ni(^{106}Cd,X) 60MeV/u	MSU	[121]
48	^{97}Cd	Sn(p,3pxn) 600 MeV	CERN	[122]
49	^{98}In	Ni(^{112}Sn,X) 63MeV/u	GANIL	[120]
50	^{100}Sn	Be(^{124}Xe,X) 1095MeV/u	GSI	[123]

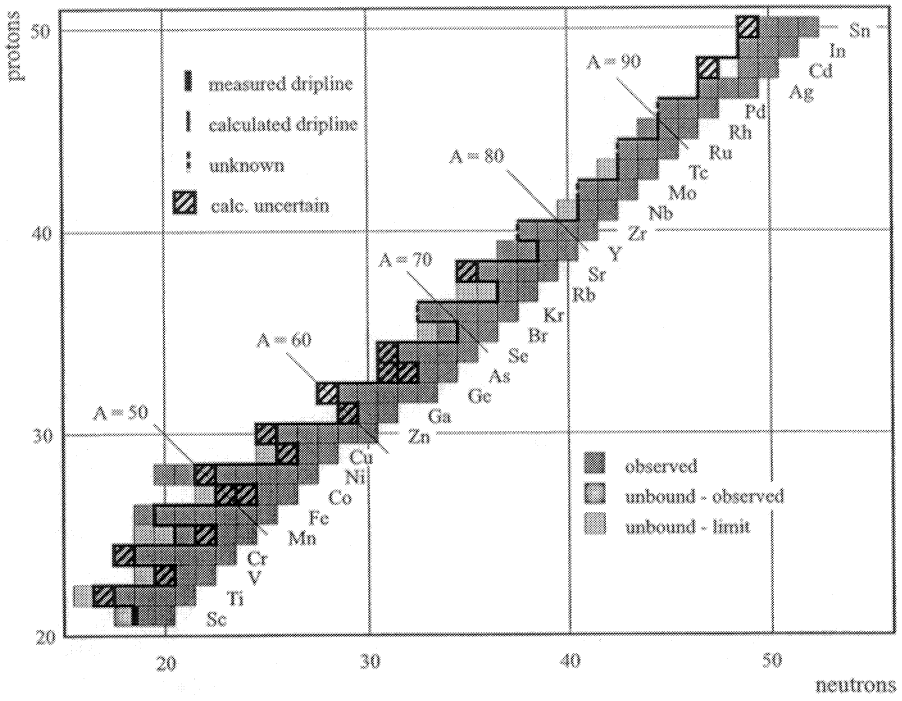

Figure 12. Nuclei at and beyond the proton dripline for $20 < Z \leq 50$.

Lifetime limits for nuclei beyond the dripline (light grey squares) were determined for ^{38}Ti [35], ^{42}V, ^{44,45}Mn [34], ^{49}Co, ^{54}Cu [127], ^{73}Rb [36], ^{81}Nb, and ^{85}Tc [119]. In addition, reference [126] adopted a lifetime limit of < 1.2 μs from the data of reference [37] for ^{68}Br and ^{72}Rb.

The only element for which the dripline has been experimentally determined is scandium, where it is located between ^{39}Sc and ^{40}Sc (doubled black line). ^{39}Sc (circled light grey square) is also the only nucleus beyond the dripline in this region of which the mass has been measured [107].

The thick solid line in the figure corresponds to the dripline extrapolated from the latest mass evaluation [105]. The striped squares show nuclei where the uncertainty of the calculated separation energy is too large to determine if the nucleus is bound or unbound. With the exception of strontium, the predictions for the even-Z nuclei between krypton and palladium do not extend beyond the dripline. The dashed line indicates the limit of the last calculated isotope, which does not necessarily have to correspond to the last bound isotope.

Experimentally, the dripline has most likely been reached for all odd-Z nuclei in this mass region. The lightest nucleus that potentially can still be bound and has not yet been observed is ^{60}Ge. It has a predicted two-proton separation energy of 48 $\pm$ 238 keV [105]. For even-Z nuclei beyond strontium the dripline has most probably not yet been reached experimentally.

4.3. Medium Mass Nuclei II: 50 < Z ≤ 82

The lifetimes for proton emission in this mass region are becoming so large for a wide range of energies that β-decays dominate for many unbound isotopes. For some elements there are 3–4 β-emitting isotopes before the proton separation energies become large enough for proton emission to compete with β-decay. Table 3 lists the lightest observed isotopes in this mass region and the reactions with which they were first observed. With the exception of $Z = 51$, all of them have been produced with fusion evaporation reactions. The table also lists the primary decay mode.

Figure 13 shows again the nuclei along the proton dripline. The notation is the same as in figure 12. With the exception of even-Z nuclei between cerium and hafnium the dripline has most likely been reached for all nuclei. The solid line again shows the extrapolated dripline derived from the AME2003 atomic mass evaluation [105], the dashed line is used for nuclei where the extrapolation does not extend towards the dripline. Experimentally the dripline has only been determined for lutetium, tantalum and gold (double black line). In addition, for thallium the dripline could be either

Table 3. Lightest presently observed isotopes for $50 < Z \leq 82$. The production reaction, observed decay, laboratory and reference of the first observation are listed.

Z	Isotope	Reaction	Decay	Laboratory	Reference
51	^{103}Sb	Ni(^{112}Sn,X) 63MeV/u	-	GANIL	[120]
52	^{106}Te	^{58}Ni(^{58}Ni,2p4n)^{110}Xe(α)	α	GSI	[128]
53	^{108}I	^{54}Fe(^{58}Ni,p3n)	α	Daresbury	[129]
54	^{110}Xe	^{58}Ni(^{58}Ni,2p4n)	α	GSI	[128]
55	^{112}Cs	^{58}Ni(^{58}Ni,p3n)	p	Daresbury	[130]
56	^{114}Ba	^{58}Ni(^{58}Ni,2n)	β	GSI	[131]
57	^{117}La	^{64}Zn(^{58}Ni,p4n)	p	Legnaro	[132]
58	^{121}Ce	^{92}Mo(^{32}S,3n)	β	Lanzhou	[133]
59	^{121}Pr	^{96}Ru(^{32}S,p6n)	β	Dubna	[134]
60	^{125}Nd	^{92}Mo(^{36}Ar,3n)	β	Lanzhou	[135]
61	^{128}Pm	^{96}Ru(^{36}Ar,p3n)	β	Lanzhou	[135]
62	^{129}Sm	^{96}Ru(^{36}Ar,3n)	β	Lanzhou	[135]
63	^{130}Eu	^{58}Ni(^{78}Kr,p5n)	p	ANL	[136]
64	^{135}Gd	^{106}Cd(^{32}S,3n)	β	Lanzhou	[137]
65	^{139}Tb	^{106}Cd(^{36}Ar,p2n)	β	Lanzhou	[138]
66	^{139}Dy	^{106}Cd(^{36}Ar,3n)	β	Lanzhou	[135]
67	^{140}Ho	^{92}Mo(^{54}Fe,p5n)	p	HRIBF	[139]
68	^{144}Er	^{92}Mo(^{58}Ni,p4n)^{145}Tm(p)	-	HRIBF	[140]
69	^{145}Tm	^{92}Mo(^{58}Ni,p4n)	p	HRIBF	[141]
70	^{149}Yb	^{112}Sn(^{40}Ca,3n)	β	Lanzhou	[142]
71	^{150}Lu	^{96}Ru(^{58}Ni,p3n)	p	Daresbury	[143]
72	^{154}Hf	^{106}Cd(^{58}Ni,2p4n)^{158}W(α)	α	GSI	[144]
73	^{155}Ta	^{102}Pd(^{58}Ni,p4n)	p	ANL	[145]
74	^{158}W	^{106}Cd(^{58}Ni,2p4n)	α	GSI	[144]
75	^{160}Re	^{106}Cd(^{58}Ni,p3n)	p	Daresbury	[146]
76	^{162}Os	^{106}Cd(^{58}Ni,2n)	α	GSI	[147]
77	^{164}Ir	^{92}Mo(^{78}Kr,p5n)	p	ANL	[136]
78	^{166}Pt	^{92}Mo(^{78}Kr,4n)	α	ANL	[148]
79	^{170}Au	^{96}Ru(^{78}Kr,p3n)	p	ANL	[136]
70	^{172}Hg	^{96}Ru(^{78}Kr,2n)	α	ANL	[149]
81	^{177}Tl	^{102}Pd(^{78}Kr,p2n)	p,α	ANL	[150]
82	^{180}Pb	^{144}Sm(^{40}Ca,4n)	α	LBL	[151]

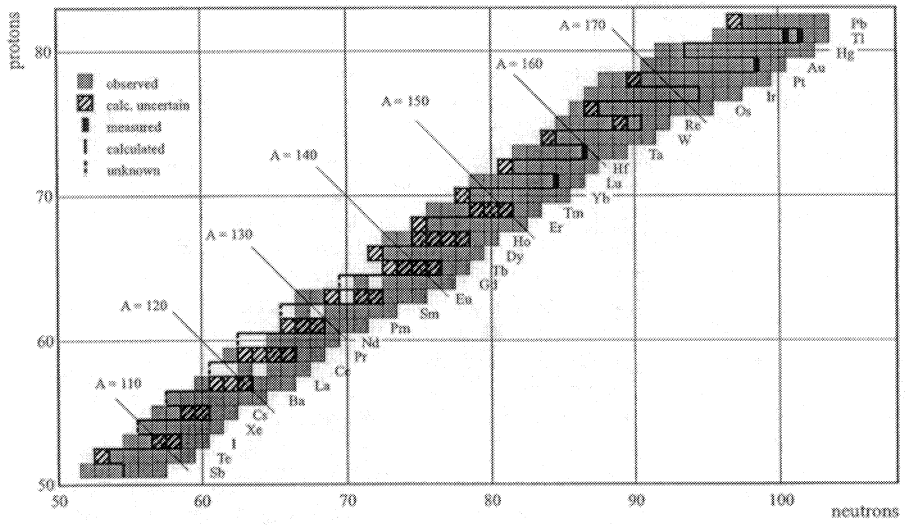

Figure 13. Nuclei at and beyond the proton dripline for $50 < Z \leq 82$.

between ^{181}Tl and ^{182}Tl or between ^{182}Tl and ^{183}Tl because the measured proton separation energy is -21 ± 77 keV for ^{182}Tl [105].

The surprisingly large uncertainty of the location of the dripline in this mass region demonstrates the fact that there is no easy signature for the dripline. The fairly shallow reduction of the separation energy as a function of isotopes requires high resolution mass measurements. For example, table 4 lists the proton separation energies for neutron deficient holmium isotopes [105]. The separation energies for $^{142-146}$Ho have to be extracted from mass measurements and extrapolations with uncertainties of hundreds of keV. In contrast, the direct observation of the proton emission of ^{141}Ho [152] and ^{140}Ho [139] allows an accurate determination of the separation energy.

The observation of ground state proton emitters which were first discovered in this mass region [153] is thus a great spectroscopic tool. However, in terms of the dripline, the discovery of proton emitters only establishes that these nuclei are beyond the dripline. The actual location of the dripline has to be determined from mass

Table 4. Proton separation energies for neutron-deficient holmium isotopes.

Isotope	S_p (keV)
140	-1094 ± 10
141	-1177 ± 7
142	-554 ± 585
143	-390 ± 540
144	+163 ± 357
145	-113 ± 300
146	+568 ± 201

measurements which are significantly more difficult.

With the recent developments in the different mass measurement techniques [154, 155] and the application of digital pulse processing [140] to access even shorter lived proton emitters the proton dripline for at least the odd-Z nuclei should be determined in the near future.

Table 4 also indicates another interesting phenomenum, i.e. the possibility that the dripline is not continuous within an isotope chain. ^{145}Ho could be unbound with ^{144}Ho being bound again. This is similar to the case of ^{9}B.

4.4. Heavy Nuclei: 83 ≤ Z

This mass region is dominated by α emitters and so far no ground-state proton emitters have been observed. Again all nuclei are populated by fusion evaporation reactions. Table 5 shows the lightest observed isotopes and the reaction with which they were first observed. It should be mentioned that proton radioactivity has been observed in this mass region from an intruder state in ^{185}Bi [170]. Also, the observations of two heaviest isotopes ^{233}Cm and ^{234}Bk have been observed only very recently [169, 168] and are the only nuclei included in the present review which have not yet been published in a refereed journal.

Figure 14 shows nuclei along the dripline up to $Z = 97$. As in figure 11 the solid line corresponds again to the experimentally determined dripline. The dripline has been reached for all odd-Z nuclei up to protactinium. The location of the dripline for even-Z nuclei is still unknown. The extrapolations [105] (dashed line) for these nuclei do not extend to negative separation energies and the dripline is most likely located towards even more neutron-deficient isotopes.

In contrast to the medium mass regions, the dripline for odd-Z nuclei is experimentally known in this mass region because most of these nuclei decay by α-emission. The accurately measured α-decay energy can be linked to more stable nuclei where high resolution mass measurements are possible.

With the possibility that ^{194}At might be bound by 117 ± 189 keV (striped square),

Table 5. Lighest presently observed isotopes for $82 < Z < 98$. The production reaction, laboratory and reference of the first observation are listed.

Z	Isotope	Reaction	Laboratory	Reference
83	^{184}Bi	^{93}Nb(^{94}Mo,3n)	GSI	[156]
84	^{188}Po	^{142}Nd(^{52}Cr,6n)	GSI	[157]
85	^{191}At	^{141}Pr(^{54}Fe,4n)	JYFL	[158]
86	^{195}Rn	^{142}Nd(^{56}Fe,3n)	JYFL	[159]
87	^{199}Fr	^{169}Tm(^{36}Ar,6n)	RIKEN	[160]
88	^{202}Ra	^{170}Yb(^{36}Ar,4n)	JYFL	[161]
89	^{206}Ac	^{175}Lu(^{36}Ar,5n)	JYFL	[162]
90	^{209}Th	^{182}W(^{32}S,5n)	JAERI	[163]
91	^{212}Pa	^{182}W(^{35}Cl,5n)	JAERI	[164]
92	^{217}U	^{182}W(^{40}Ar,5n)	JINR	[165]
93	^{225}Np	^{209}Bi(^{20}Ne,4n)	JINR	[166]
94	^{228}Pu	^{208}Pb(^{24}Mg,4n)	JINR	[167]
95	^{230}Am	^{197}Au(^{40}Ar,3n)^{234}Bk(α)	RIKEN	[168]
96	^{233}Cm	^{198}Pt(^{40}Ar,5n)	GSI	[169]
97	^{234}Bk	^{197}Au(^{40}Ar,3n)	RIKEN	[168]

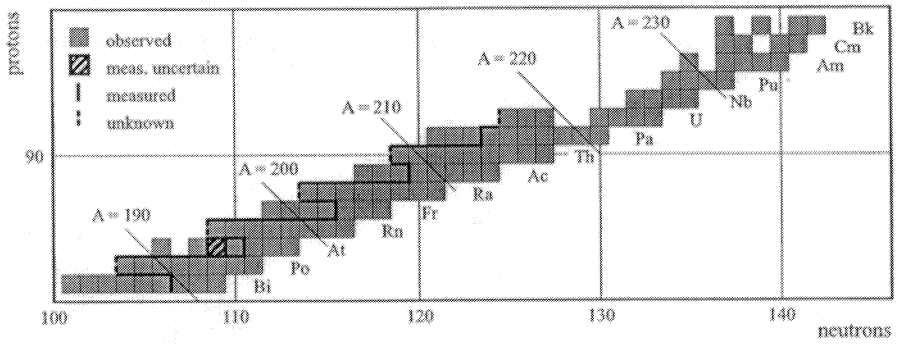

Figure 14. Nuclei at and beyond the proton dripline for $82 < Z < 98$.

^{195}At could be an unbound nucleus (S_p = -234 ± 15 keV) surrounded by bound nuclei.

For nuclei beyond uranium, the dripline is out of reach for all nuclei. However, it should be mentioned that in the region of the superheavy nuclei ($Z > 110$) the produced nuclei are again closer to the dripline [171].

4.5. Predictions of the Proton Dripline

The location of the driplines is directly related to the nuclear masses determined by equations 4 and 5. A recent review compared the predictive power of the commonly used global mass models in detail [155]. Thus the different models will not be discussed here and only a few representative models will be compared to demonstrate the theoretical uncertainties in the prediction of the proton dripline. It should be mentioned that the dripline can be calculated fairly accurately from the binding energies of analog neutron-rich nuclei and Coulomb energy shifts [172]. However, this method can only be applied in mass regions ($Z \lesssim 30$) where the binding energies of the analog nuclei are well known.

Figure 15 shows the deviations of the empirical model based on p-n interaction by Tachibana *et al.* (TUYY) [18], the finite-range droplet model (FRDM) [173], and the Hartree-Fock-Bogolyubov model (HFB-2) [174] from the extrapolated masses of the AME2003 atomic mass evaluation [105]. The agreement of the three models is quite good over the whole chart of nuclei. The figure shows the deviations for the odd-Z (top) and the even-Z (bottom) nuclei separately.

With a few exceptions the dripline for odd-Z nuclei is reproduced within one neutron up to tin. Even beyond tin up to lutethium the deviations are not more than two neutrons. Considering that the uncertainty of the extrapolated dripline in this region can be as large as four neutrons (see table 4) these deviations are probably not significant. The mean standard deviation of the models for known masses is on the order of a few hundred keV [155].

The calculations seem to be even better for the even-Z nuclei. Neither of the models deviates by more than two neutrons all the way up to lead. With the exception of the HFB-2 model in the heavy mass region, most of the deviations are towards negative values which is due to the fact that for many of the even-Z isotopes the mass evaluation does not extrapolate to negative separation energy. This suggests that

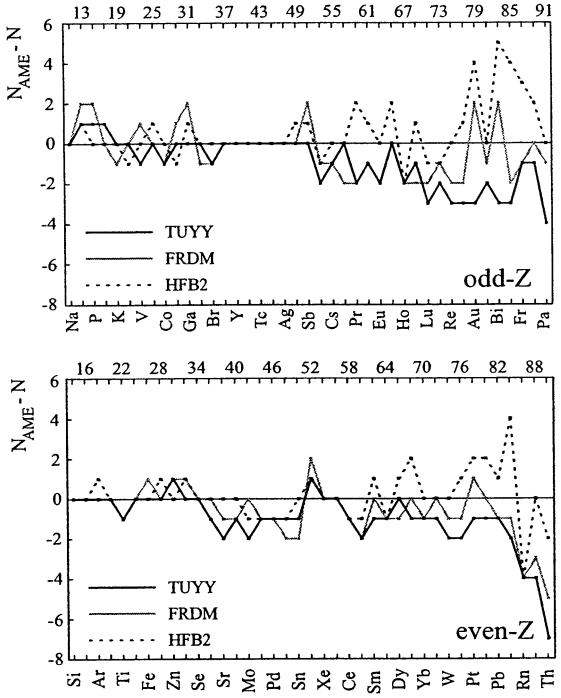

Figure 15. Difference of the calculated location of the dripline for odd-Z (top) and even-Z (bottom) nuclei between the extrapolation by the recent mass evaluation N_{AME} ([105]) and the three mass models indicated in the figure.

the predictions of these models are probably correct and that the dripline is actually located at even more neutron-deficient isotopes.

Even the large deviation of 4–6 neutrons beyond lead are most likely due to the limited extrapolation. Figure 2 of reference [175] shows that the known two-proton separation energies for even-even nuclei in this mass region do not extend to the proton dripline.

4.6. Exotic Decay Modes

Ground-state two-proton radioactivity has been predicted already in 1960 [22]. This decay can occur in even-Z nuclei beyond the proton dripline where the pairing energy between the last two protons causes the one-proton decay channel to be energetically forbidden or at least strongly hindered. The emission of the two protons can theoretically proceed through several mechanisms [176, 177]. The simultaneous correlated emission of a "di-proton" competes with the direct three-body breakup and the sequential binary decay if energetically possible. Searches for short-lived ground state "di-proton" emitters in the light mass region as well as for real two-proton radioactivity in medium mass nuclei have been unsuccessful [13] until recently.

Several theoretical calculations predicted that the best candidates for two-proton

radioactivity were ^{45}Fe, ^{48}Ni and ^{54}Zn [20, 178, 172]. Finally, in 2002, over 40 years after the initial prediction evidence for this exotic decay was reported for ^{45}Fe [124, 125].

Figure 16 shows the one-proton and two-proton separation energies for the $N = 19$ isotones (top) and the relations between ^{45}Fe, ^{44}Mn and ^{43}Cr (bottom) as calculated within HFB-2 [174]. The figure shows that the pairing effect is responsible for the possible occurrence of two-proton radioactivity. While the decrease of the two-proton separation energy towards the dripline is smooth, the one-proton separation energy is larger for even-Z nuclei compared to odd-Z nuclei towards the dripline. When the crossing of S_p and S_{2p} occurs at the dripline the nucleus (^{45}Fe) is bound with respect to one-proton emission but unbound with respect to two-proton emission.

The recent experiments did not observe the individual protons, so that the exact decay mode of ^{45}Fe is not clear. In order to rule out direct three-body breakup, the angular correlation of the two emitted protons has to be measured. The sequential emission of two protons depends critically on the one proton separation energy of ^{45}Fe. In all previous two-proton emission experiments where intermediate states were energetically allowed, no evidence for correlated emission was observed [87, 106, 179, 180, 181].

The one-proton separation energy of 180 keV shown in figure 16 seems to indicate that for ^{45}Fe the sequential decay channel is clearly not open. The AME2003 [105] quotes a similar value of 110 keV, however, it has a large uncertainty of 550 keV. The more detailed calculations predict the single proton separation energy to be between

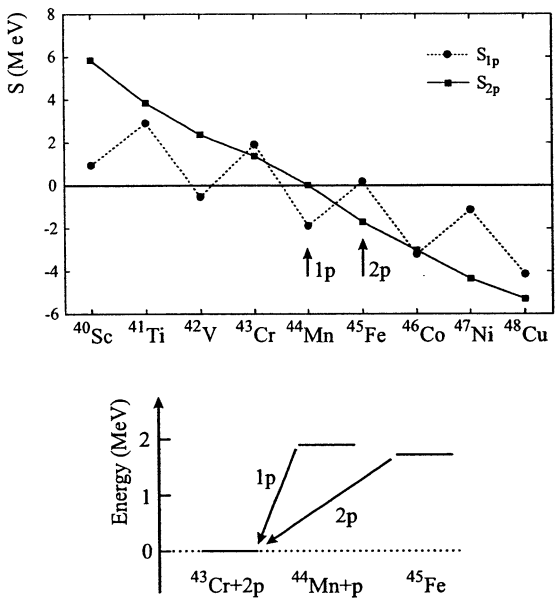

Figure 16. One-proton (·····) and two-proton (——) separation energies for $N = 19$ isotones (top). Decay scheme for the potential two-proton emitter ^{45}Fe (bottom).

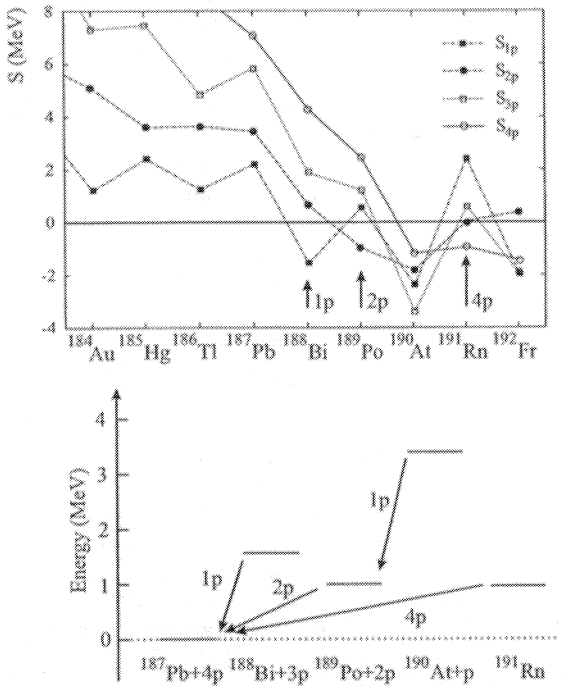

Figure 17. One- (— · —), two- (- - -), three- (·····) and four-proton (——) separation energies for $N = 102$ isotones (top). Decay scheme for the potential two- (^{186}Po), three- (^{187}At), and four-proton emitter (^{188}Rn) (bottom).

-24 keV and 10 keV [20, 178, 172]. Even if ^{45}Fe is unbound with respect to one proton emission, the very small decay energy would lead to an extremely long lifetime for this decay mode. Thus, ^{45}Fe is an ideal case to finally observe di-proton emission.

Two proton radioactivity is so rare and hard to observe because the energy window for this is rather small. It is a delicate balance between a decay energy which is too high, leading to an unobservable fast decay on the one hand and a too low decay energy, making the decay so slow that it cannot compete with β^+ emission. In addition to the efforts in the Fe/Ni region, there is currently significant interest in the potential two-proton emission of ^{19}Mg [89, 104, 182]

Since it took over 40 years to observe two-proton radioactivity, one might speculate that even more exotic decays could exist and could be observed eventually.

As an example Figure 17 shows the one-, two-, three- and four-proton separation energies of the $N = 105$ isotones (top) and the relations between the decay energies of ^{191}Rn, ^{190}At, ^{189}Po, ^{188}Bi and ^{187}Pb (bottom) as calculated with the HFB-2 model. In addition to the pairing effect influencing the one- and three-proton separation energies, the two-proton separation energy is predicted to increase for ^{191}Rn and ^{192}Fr. Thus, for ^{191}Rn, the one-, two, and three-proton separation energies are positive, while the four-proton separation energy is negative. This could potentially result in an emission of a four-proton cluster. This particular case is unrealistic because already ^{188}Bi has

been measured to be an α emitter and the two-proton separation energy of ^{189}Po is positive. However, figure 17 demonstrates that the interplay of the different nuclear forces can lead to surprising results for the multi-proton separation energies and in the region well beyond the dripline very exotic decay modes might exist.

Even if the emission of a four-proton cluster is very unlikely, the sequential emission of two or more protons similar to the α-decay chains could become observable once even-Z nuclei significantly beyond the proton dripline become accessible.

5. Neutron Dripline

The first exotic nucleus observed on the neutron-rich side was ^{16}C [183] with a (t,p) reaction on a radioactive ^{14}C target. An exotic nucleus is here defined as a nucleus that is more than one proton or neutron away from the valley of stability.

Figure 18 shows the chart of nuclei for stable and neutron-rich nuclei up to calcium $Z = 20$. Stable nuclei are shown in black, bound nuclei in dark-grey and unbound nuclei in light-grey. For the circled light grey unbound nuclei spectroscopic measurements have been performed. The experimentally determined dripline is shown by the thick black line. The dashed line shows the most likely location of the dripline, but which has strictly speaking experimentally not been confirmed. The dashed squares are nuclei which could be either bound or unbound based on the uncertainties of the AME2003 extrapolations [105]. The grey line shows the dripline as predicted by the mass model of Tachibana *et al.* [18].

In the present review only nuclei up to $Z = 20$ (calcium) will be discussed, because beyond calcium the dripline diverges significantly from the reach of current accelerators.

Following the usual description of the neutron dripline in terms of elements, it is commonly believed that the neutron dripline has been reached for all elements up to oxygen. The last dripline nucleus is ^{24}O which was already discovered in 1970 [63]. If

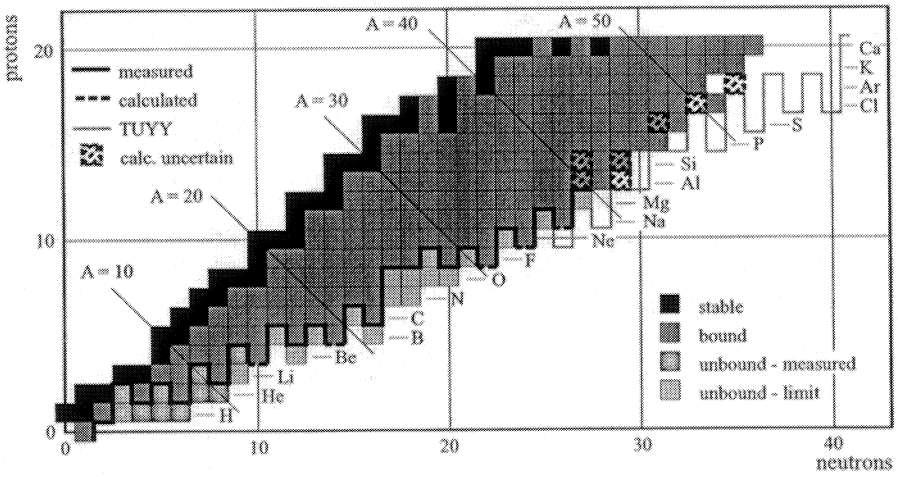

Figure 18. Nuclei at and beyond the neutron dripline for $Z \leq 20$.

it turns out that ^{31}F is the last stable fluorine isotope [184], it will have taken almost 30 years to push the dripline limit from $Z = 8$ to $Z = 9$.

However, the observation of a certain isotope is not sufficient to determine the location of the dripline. In addition it is necessary to prove that the next isotope is unbound and thus beyond the dripline. If the neutron dripline is discussed in terms of elements even this is not sufficient. In order to show that ^{24}O represents the dripline, it had to be shown that ^{25}O [29], ^{26}O [31] and even ^{28}O [185], which had been predicted to be bound due to the shell effects, are unbound.

As mentioned in section 2.4 it is more appropriate to discuss the neutron dripline in terms of isotones, just like the proton dripline was discussed in terms of isotopes.

5.1. Isotones with $N \leq 8$

According to the above definition, the first exotic dripline nucleus observed was ^{8}He [186]. With a neutron to proton ratio of 3, ^{8}He can also be considered the most neutron-rich bound nucleus. The location of the dripline was then established for the isotones $4 \leq N \leq 8$ with the "non-observation" of ^{5}H [27], ^{7}He [52], ^{7}H [187], ^{10}Li and ^{10}He [52]. With the dripline so close to the valley of stability, spectroscopic measurements were also performed for these nuclei. From the width of the measured resonances lifetimes of $>$ 1.3 zs (^{5}H, [188]), 4.4 zs (^{7}He, [189]), 0.022 zs (^{7}H, [83, 126]), $>$ 2.9 zs (^{10}Li, [190]) and 3.9 zs (^{10}He [84]) were extracted (1 zs = 10^{-21} s). With the exception of ^{7}H these nuclei have lifetimes which are long compared to the nuclear time scale ($\sim 10^{-22}$s) and should be considered nuclei. The resonance parameters for ^{5}H are still controversial [191, 192]. The lifetime for ^{7}H of 2.2 $\cdot 10^{-23}$s was extracted from an estimated peak width of 20 MeV [126] and was not quoted in the original paper [83]. Within the present definition of a nucleus ^{7}H certainly does not qualify.

Spectroscopic measurements were even performed on ^{6}H [75, 193] and ^{9}He [74, 194]. In addition to ^{4}H [192] these are presently the only measured nuclei within an isotone chain which are removed from the dripline by two nucleons.

The discussion if these extremely short-lived nuclei can be viewed as nuclei at all has to address another issue concerning unbound nuclei beyond the neutron dripline. In absence of the Coulomb barrier, the only force holding an unbound neutron to the nucleus is the centrifugal force due to the angular momentum. For nuclei between 2 $< N \leq 8$ the last neutron should fill the p-shell, i.e. have an angular momentum of one. The angular momentum barrier for an $l = 1$ neutron and a decay energy smaller than $\sim$1 MeV results in lifetimes of the order of 10^{-21}s (see also figure 5).

However, already in 1960 Talmi and Unna explained the spectrum of ^{11}Be [195] by an inversion of the 1p-shell with the 2s-shell. This level inversion is not an isolated occurrence but continues for $N = 7$ isotones beyond the dripline [70, 194, 196]. The unbound neutron in the ground state of ^{10}Li and ^{9}He is in the s shell and has zero angular momentum. Thus, there is no barrier which prevents the neutron from being emitted. The definition of a lifetime based on the width of a resonance is not valid anymore. These nuclei can only be described as scattering states, or virtual resonances.

The most famous dripline nucleus is probably ^{11}Li. The initial assumption that it was unbound lead to a misidentification of ^{12}Be [51]. ^{11}Li, together with ^{14,15}B was first observed in a spallation reaction [52]. The lifetime of 8.5$\pm$1 ms was first measured in 1969 [56]. However, it was the observation of its unexpected neutron halo structure [197] that sparked the tremendous interest in the field of exotic nuclei. The structure and nature of the halo in ^{11}Li has since been studied extensively (see for

example reference [198] and reference therein).

Following the observation of ^{11}Li as a two-neutron halo, many other neutron-rich nuclei for example ^{12,14}Be and ^{19}C have been identified as two-neutron halos (see references in [11]). ^{14}Be can even be viewed as a four-neutron halo with a ^{10}Be core. The breakup of ^{14}Be into ^{10}Be and four neutrons has been measured and resulted in the surprising evidence for the observation of a four-neutron cluster structure [199].

5.2. Isotones with $8 < N \leq 20$

Initially the dripline was first explored with proton spallation reactions, however, starting from $N = 14$, projectile fragmentation is essentially the only method to explore the dripline. Table 6 shows the nuclei at and beyond the dripline together with production mechanism of the first observation, or non-observation. Although ^{28}F was stated as being unbound in reference [200] it was not explicitly shown. However, later it was confirmed that ^{28}F is indeed beyond the neutron dripline [184]. ^{13}Be is presently the heaviest neutron unbound nucleus where spectroscopic information has been measured [72].

As can be seen from table 6 the dripline has not been unambiguously measured for $N = 10$. Although not observed in the data of references [32, 202], the authors could not conclusively determine that ^{13}Li was unbound. Thus, strictly speaking, the neutron dripline has only been established up to $N = 9$. Again, at $N = 14$, the non-existence of ^{18}Be has not been shown. However, extrapolations of the existing surrounding nuclei make it very unlikely that either of these two nuclei (^{13}Li, ^{18}Be) are bound. Otherwise the neutron dripline has been mapped very well in this mass region.

The most interesting feature of the dripline in this mass range is the change of the shell structures. The inversion of the p and s shell for the ground states of the $N = 7$ isotones close and beyond the dripline reflects the disappearance of the $N = 8$ shell gap. It was a first indication that the classical shell structure derived from properties of nuclei along the valley of stability changes significantly for neutron-rich nuclei.

The disappearance of the $N = 20$ shell at the dripline is responsible for the fact

Table 6. Last bound and first unbound isotones along the neutron dripline for $8 < N \leq 20$. The nuclei are produced by target spallation (SP) or projectile fragmentation (PF). The production reaction and reference of the first observation are listed.

N	Bound	Reaction	Reference	First Unbound	Reaction	Reference
9	^{14}B	SP	[52]	^{13}Be	SP	[53]
10	^{14}Be	SP	[32]	—		
11	^{17}C	SP	[53]	^{16}B	SP	[32]
12	^{17}B	SP	[32]	^{16}Be	PF	[201]
13	^{19}C	SP	[202]	^{18}B	PF	[203]
14	^{19}B	PF	[203]	—		
15	^{22}N	PF	[204]	^{21}C	PF	[29]
16	^{22}C	PF	[205]	^{21}B	PF	[206]
17	^{26}F	PF	[204]	^{25}O	PF	[29]
18	^{27}F	PF	[28]	^{26}O	PF	[31]
19	^{29}Ne	PF	[29]	^{28}F	PF	[184]
20	^{29}F	PF	[200]	^{28}O	PF	[185]

that the otherwise double magic nucleus ^{28}O is unbound. Even ^{26}O is not bound. It should be mentioned that as early as 1970 it was predicted that, contrary to other calculations [207, 208] ^{24}O should be the last particle stable oxygen isotope [63].

The first evidence of the unbound character of ^{26}O was reported in 1990, however, the same measurement also concluded that ^{31}Ne would be unstable [31]. In 1996 it was confirmed that ^{26}O was indeed unbound [209].

The question of the instability of the ^{26}O and ^{28}O resulted in a detailed survey of this mass region. For the three isotones $17 < N < 19$ the instability of nuclei with two neutrons away from the dripline was reported with ^{24}N [205], ^{25}N, and ^{27}O [184]. Indications for the instability of ^{27}O [185] had been reported in the search for ^{28}O.

Connected with the disappearance of the $N = 20$ shell gap is the appearance of a new gap at $N = 16$. A survey of neutron separation energies, in addition to other evidence, showed clearly the emergence of a new shell gap for oxygen isotopes at $N = 16$ [210]. In a plot of two-neutron separation energies the shift of the gap from $N = 20$ to $N = 16$ can be seen [211]. Another indication for the existence of this shell is the fact that $N = 16$ corresponds to the last bound nucleus not only for oxygen (^{24}O) but also for nitrogen (^{23}N) and even carbon (^{22}C). It has been speculated that because of this shell gap ^{21}B might be bound. However, a recent experiment could not find any evidence for the existence of ^{21}B [206].

There are also experimental indications that another gap exists for $N = 14$ [212]. The existence of ^{19}B could be evidence for additional binding due to this gap. However, it also might be a motivation to search for the potential existence of ^{18}Be.

The disappearance and appearance of these shells along the neutron dripline can be accounted for by recent shell model calculations [213]. In the near future more spectroscopic data of unbound nuclei beyond beryllium should become available, which would solidify the shell model calculations.

5.3. Isotones with $N > 20$

The dripline for odd-N nuclei has experimentally unambiguously been determined up to $N = 27$. The heaviest observed dripline nucleus up to date is probably ^{43}Si or maybe even ^{46}P. For even-N nuclei the location of the dripline has not been established beyond $N = 20$ although it is very unlikely that ^{30}O could be bound. Table 7 lists the bound and unbound isotones for $20 < N \leq 36$.

The present approach to question the unbound character of ^{30}O seems extreme. However, extrapolations from known properties to predict the location of the dripline are unreliable. For example, the measured very short β-decay half-life of ^{35}Na of 1.5 ms [58], which is the shortest β-decay half-life measured so far, lead to the assumption that ^{37}Na should be unbound. Nevertheless, it was subsequently observed to be bound [214, 215]. The mass measurement of ^{41}Si [216] corresponds to a negative one-neutron separation energy of -20 ± 1930 keV [105]. Although this value is consistent with the observation that ^{41}Si is bound [200], one would expect ^{43}Si to be unbound (-190 ± 860 keV, [105]). However, ^{43}Si is also bound [214].

The question where the dripline is located for $N = 24$ is the same as where the dripline is located for $Z = 9$, i.e. is ^{33}F bound or not. If it is bound it would be the first case on the neutron-rich side where a gap in an isobar chain occurs (^{33}Na is unbound). These gaps certainly do exist for heavier masses along the neutron dripline and it is just a question for which mass it occurs for the first time. Along the proton dripline such gaps appear for the first time for masses above $A = 40$.

Table 7. Last bound and first unbound isotones along the neutron dripline for $20 < N \leq 36$. The nuclei are produced by target spallation (SP), projectile fragmentation (PF), or projectile fission (FI). The production reaction and reference of the first observation are listed.

N	Bound	Reaction	Reference	First Unbound	Reaction	Reference
21	^{31}Ne	PF	[33]	^{30}F	PF	[184]
22	^{31}F	PF	[184]	—		
23	^{34}Na	SP	[58]	^{33}Ne	PF	[214, 215]
24	^{34}Ne	PF	[214, 215]	—	PF	
25	^{37}Mg	PF	[33]	^{36}Na	PF	[214, 215]
26	^{37}Na	PF	[214, 215]	—		
27	^{40}Al	PF	[217]	^{39}Mg	PF	[214]
28	^{41}Al	PF	[217]	—		
29	^{43}Si	PF	[214]	—		
30	^{45}P	PF	[218]	—		
31	^{46}P	PF	[218]	—		
32	^{48}S	PF	[218]	—		
33	^{51}Ar	PF	[200]	—		
34	^{51}Cl	PF	[218]	—		
35	^{54}K	SP	[58]	—		
36	^{56}Ca	FI	[76]	—		

The next interesting question regarding the location of the dripline in this mass region is the presence of the $N = 28$ shell gap. Will the gap persist towards the dripline and influence the stability of ^{40}Mg and ^{39}Na? Evidence for a weakening of the shell gap has been reported for neutron-rich nuclei not located directly at the dripline [216, 219, 220]. Most global mass models (see for example references [18, 173, 174]) as well as the AME2003 [105] predict ^{40}Mg to be bound. The non-observation of ^{40}Mg would thus be additional strong evidence for the weakening of the $N = 28$ shell at the neutron dripline.

For nuclei beyond the $N = 28$ shell the dripline may have been reached for the odd-N nuclei but certainly not for the even-Z nuclei. While a few more dripline nuclei will be produced in the near future, major advances will have to wait for second generation radioactive beam facilities (see section 7).

5.4. Predictions of the Neutron Dripline

Since the driplines will not be accessible much beyond $N \sim 28$ in the near future the predictions of the neutron dripline for heavier nuclei by the different mass models can not be tested. Thus they will be discussed here only briefly.

Figure 19 shows the neutron dripline for the same global models presented for the proton dripline: the empirical model by Tachibana *et al.* TUYY [18], the finite-range droplet model (FRDM) [173], and the Hartree-Fock-Bogolyubov model (HFB-2) [174]. In order to show the differences between the models the curves are offset with respect to each other by their linewidths.

The valley of stability on the neutron-rich side is much shallower than on the proton-rich side (See figure 3). Thus assuming the same uncertainties in the models the uncertainty of the location of the neutron dripline covers a larger range of neutrons.

In order to compare the models more quantitatively, the difference of the FRDM and the HFB-2 from the TUYY model were calculated. A comparison with the

AME2003 as was done for the proton dripline in figure 15 is not possible because the heaviest extrapolation for a nucleus beyond the neutron dripline is for ^{49}S. First, the differences are shown in the usual description of the dripline as a function of Z.

Figure 20 shows deviations of up to 15 neutrons for the location of the dripline which is significantly worse than the deviations for the proton dripline. However, as has been mentioned already before, the location of the dripline as a function of Z is problematic. Because of the odd-even staggering due to the pairing effect it is hard

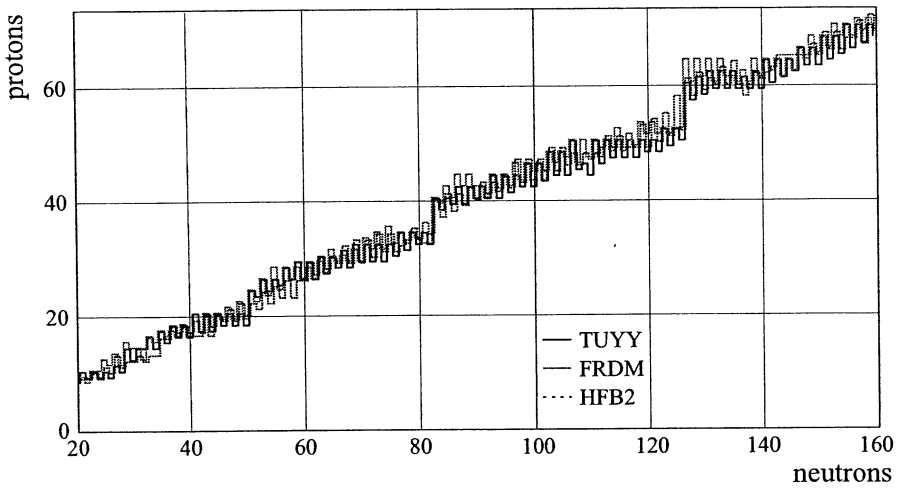

Figure 19. Neutron dripline predicted by the mass models indicated in the figure.

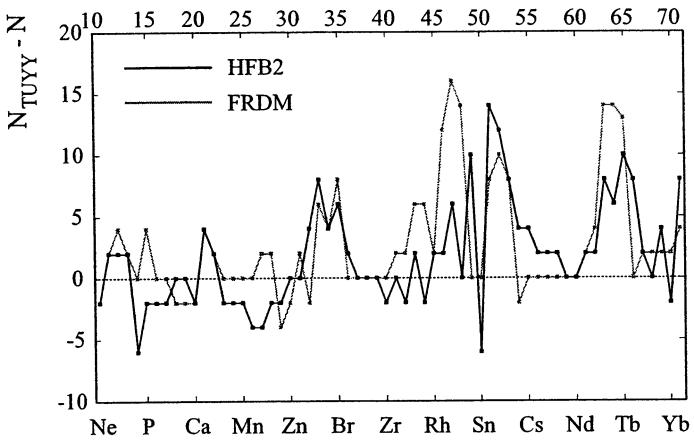

Figure 20. Difference of the calculated location of the first isotope beyond the dripline between the mass model of Tachibana, Uno, Yamada, and Yamada (TUYY) and the two other mass models indicated in the figure.

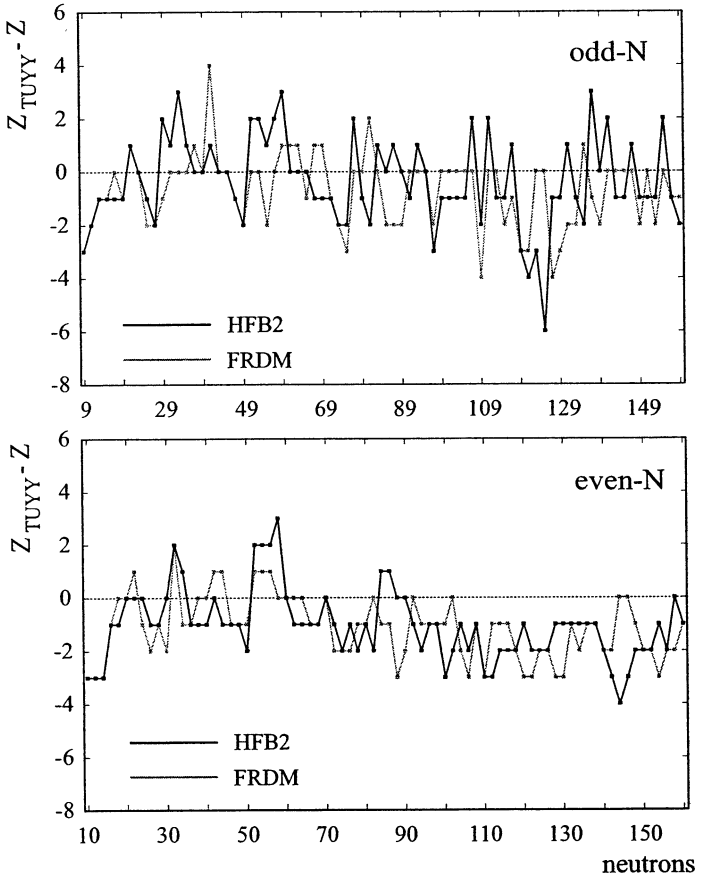

Figure 21. Difference of the calculated location of the dripline for odd-N (top) and even-N (bottom) nuclei between the mass model of Tachibana, Uno, Yamada, and Yamada (TUYY) and the two other mass models indicated in the figure.

to define the exact location of the dripline. For figure 20 the dripline was defined as the first occurance of an unbound nucleus.

To be consistent with the proton dripline, the deviations of the neutron dripline between the models should be displayed as a function of N. Figure 21 shows these differences for odd-N (top) and even-N (bottom) nuclei. In this presentation the location of the dripline is fairly well defined. There may be a few exceptions where an unbound nucleus is surrounded by bound nuclei. The effect also can potentially occur on the proton dripline as was mentioned for example for ^{145}Ho and ^{194}At.

Figure 21 shows surprisingly good agreement between the models. On the average the deviations are less than 3 protons (note the change of scale relative to figure 20). A larger deviation between the HFB-2 and the TUYY model occurs close to the $N = 126$ shell closure.

Thus the differences between the model calculations for the location of the neutron

dripline are not as large as commonly believed.

5.5. Exotic Structures and Decay Modes

Even though the di-neutron is unbound it has been speculated that even larger neutron clusters might be bound. The existence of a ^{3}n has been reported in 1965 [221] which started speculation about the stability of ^{4}n [222].

This discussion was recently started again by an observation of four neutrons in the breakup of ^{14}Be into ^{10}Be. It was claimed that the data were consistent with a four neutron cluster and all other possible background events were ruled out [199]. However, this observation has not been confirmed.

In addition to the search for large neutron clusters, a simple but exotic decay would be neutron radioactivity. In absence of the Coulomb barrier, neutron radioactivity has to rely on the angular momentum barrier. Even large angular momenta will open up only a narrow energy window for the unbound nucleus to exhibit significant lifetimes. Unfortunately, larger angular momentum states at the dripline are populated only in heavier nuclei which are currently and maybe even in the future out of reach.

Another possibility is the di-neutron decay. The di-neutron decay has the advantage over the di-proton decay, that even for the smallest decay energies the lifetimes will be small compared to β-decay lifetimes. The decaying nucleus still has to be bound with respect to one neutron emission and the width of this intermediate state has to be narrow in order to rule out sequential two neutron emission. The relation between the one- and two-neutron separation energies and the decay schemes is equivalent to the di-proton emission shown in figure 16.

It might be that already ^{16}Be is a di-neutron emitter. ^{16}Be is extrapolated [105] to be bound with respect to one-neutron emission by 191 $\pm$ 711 keV and unbound with respect to two-neutron emission by -1581 $\pm$ 520 keV.

Essentially all of the even-N nuclei along the dripline could be di-neutron emitters depending of course on the ground-state properties of the intermediate state. All three mass models chosen as examples for this review predict ^{42}Mg to be a di-neutron emitter [18, 173, 174]. In addition, ^{33}F [18], ^{36}Ne, and ^{39}Na [174] could also decay by emitting a correlated di-neutron.

Of course, if di-neutron emission is possible one can also speculate about the tetra-neutron emission. Even if the free tetra-neutron is not confirmed, the possibility for the emission of a correlated four-neutron cluster from a neutron-rich nucleus is not excluded. The FRDM does indeed predict ^{38}Ne and ^{44}Mg to be unbound with respect to four-neutron emission but bound with respect to one-, two- or three-neutron emission. Although these nuclei are necessarily four neutrons beyond the dripline, they might be in reach for future generation facilities.

6. Astrophysical Implications

The importance of the understanding of nuclei along the driplines for the astrophysical rapid proton capture process (rp-process) and the rapid neutron capture process (r-process) is currently one of the most interesting problems in nuclear physics. There are excellent reviews [223, 224] and the details of these processes will not be described here. Actually, in the following it will only been shown that the location of the driplines themselves bear very little importance for these processes. This does not mean that

the nuclear structure of the nuclei at and even beyond the dripline are not extremely important for the rp- and the r-process.

6.1. rp-process

The rp-process is responsible for powering stellar explosions such as X-ray bursts and follows very closely the proton dripline. It consists of a combination of radiative proton capture reactions (p,γ) and β-decays. Waiting points occur when the (p,γ)/β sequence reaches the proton dripline and the last nucleus at the dripline has a long lifetime. The lifetimes of the waiting point nuclei determine the duration of the rp-process and the shape of the X-ray burst light curves.

Although very closely related to the rp-process, the exact location of the dripline is not relevant. Figure 22 shows as an example the situation for the waiting point nucleus ^{68}Se. The figure depicts three different scenarios for the separation energy of ^{69}Br: (a) $S_p < 0$, (b) $S_p = 0$, and (c) $S_p > 0$. In all cases it is assumed that ^{70}Kr is bound with respect to one- and two-proton emission, which is a reasonable assumption for all even-Z nuclei along the rp-process path.

If ^{69}Br is unbound, a minimum proton energy (equal to S_p) is necessary in order

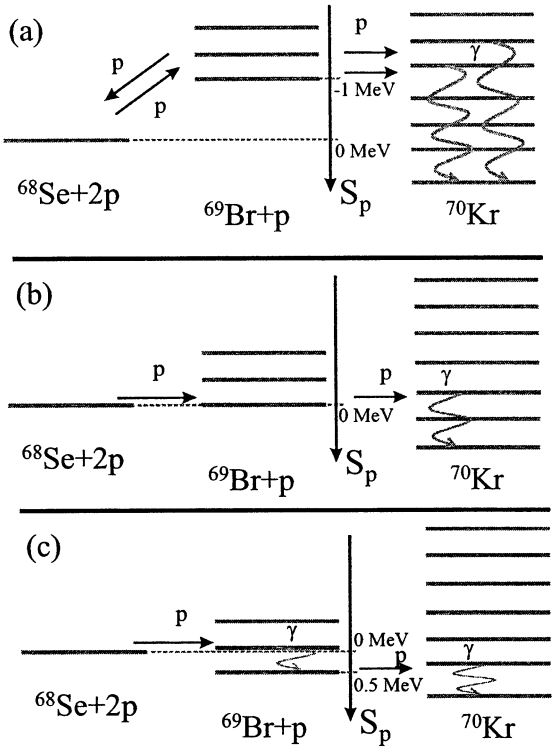

Figure 22. Possible decay schemes involving the rp-process waiting nucleus ^{68}Se, assuming: (a) $S_p < 0$, (b) $S_p = 0$, and (c) $S_p > 0$ for ^{69}Br.

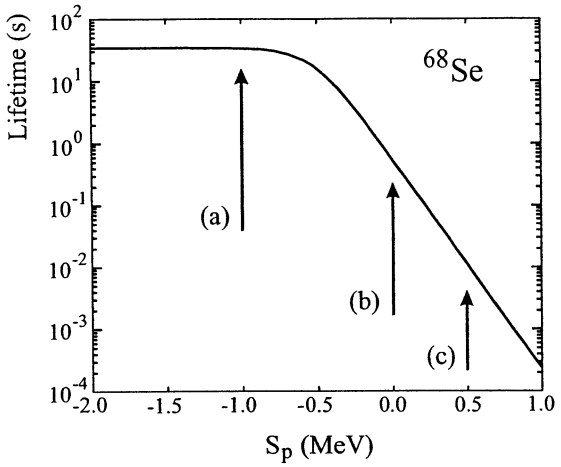

Figure 23. Stellar lifetime of ^{68}Se as a function of the ^{69}Br proton separation energy S_p (adapted from reference [223]). The arrows refer to the energy schemes of figure 22.

for the first capture reaction to proceed. This initial reaction can either be followed by a second proton capture populating ^{70}Kr, or the proton can be re-emitted decaying back to ^{68}Se. The initial capture cross section decreases with increasing separation energy and the probability to decay back increases as the separation energy increases. Both effects reduce the probability of bridging the waiting point by sequential two proton capture.

On the other hand, if ^{69}Br is bound, no minimum energy is required and the direct proton capture can populate states in ^{69}Br which cannot or are very unlikely to decay back to ^{68}Se. Thus, once captured, ^{69}Br will deexcite to its ground state where it can capture the second proton to continue the rp-process to heavier masses.

The situation where $S_p = 0$ is not a singularity and has no special significance as it applies to the stellar lifetime. For low temperatures (T < 2 GK) during the rp-process the total decay width for a waiting point nucleus with proton number Z is given by [223]:

$$\lambda_{total} = \lambda_{\beta(Z)} + g(T) * e^{S_p/kT} * < p\gamma >_{Z+1} \quad (6)$$

The overall stellar lifetime of ^{68}Se ($\tau_{Stellar} = \hbar/\lambda_{total}$) in this environment depends on the β-decay width of ^{68}Se ($\lambda_{\beta(Z)}$) and the proton capture rate on ^{69}Br. g(T) is a smooth function of temperature. The most important parameter is the exponential factor.

Figure 23 shows the overall stellar lifetime of ^{68}Se at a temperature of 1.5 GK and a density of 10^6 g/cm^3. The figure was adapted from the review by Schatz *et al.* [223]. The three arrows indicate the location of the three scenarios of figure 22. It is obvious that there is nothing special about the point $S_p = 0$. The overall lifetime of the waiting point nucleus already begins to decrease while the intermediate nucleus ^{69}Br is still unbound. The actual crossing of the dripline is just an undistinguishable point along the decreasing lifetime.

Nevertheless it is crucial to measure the masses of all three nuclei involved (^{68}Se, ^{69}Br and ^{70}Kr) in order to determine if a particular nucleus (^{68}Se) is a waiting point along the rp-process path.

6.2. r-process

The r-process is the equivalent process on the neutron-rich side. It consists of a rapid succession of radiative neutron capture processes until it reaches very neutron rich nuclei where the (n,γ) process is in equilibrium with the inverse (γ,n) process, at which point it continues by β-decay [224, 225, 226]. The r-process follows approximately a path along nuclei for which the neutron binding energy is $\sim$ 2–4 MeV.

Figure 24 shows a possible r-process path, assuming it follows along nuclei with neutron separation energies of 3 MeV, for the three different global mass models used as examples in this review.

The figure demonstrates the importance of the detailed nuclear structure. The question of the disappearance of the standard shell gaps and the possible emergence of new gaps is crucial for the r-process path. Nuclei with neutron shell gaps are waiting points for the r-process because the separation energy for the next isotope beyond the magic number is small and the lifetimes of the shell gap nuclei are long. If the shell gaps vanish, the waiting points disappear and the path changes significantly resulting in different distributions of the final abundances [227].

The discussion of the neutron dripline in terms of neutron numbers chosen in this review is not adequate for the r-process. The r-process follows isotopic chains via the neutron capture reactions. The balance between (n,γ) and (γ,n) reactions occurs for nuclei with the same Z. The r-process proceeds via β-decay as soon as the neutron separation energy drops significantly below 3 MeV (for the current example). Thus,

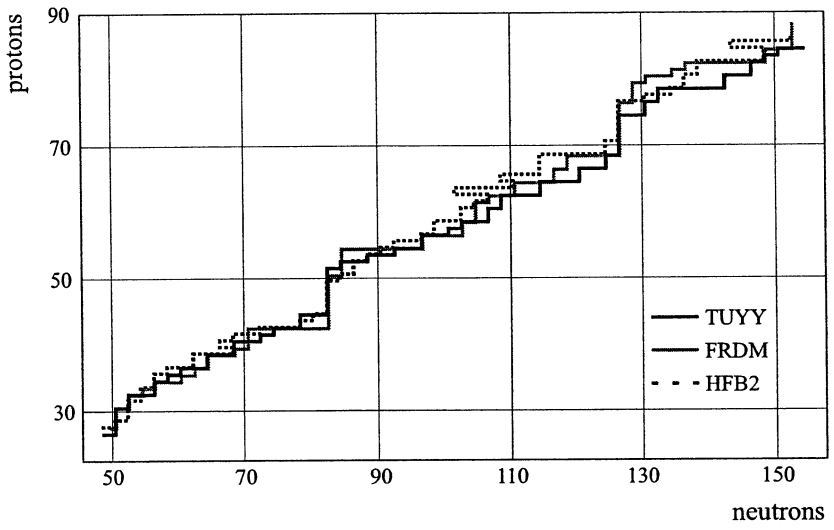

Figure 24. Location of the r-process assuming a path of nuclei with S_n = 3 MeV as predicted by the mass models indicated in the figure.

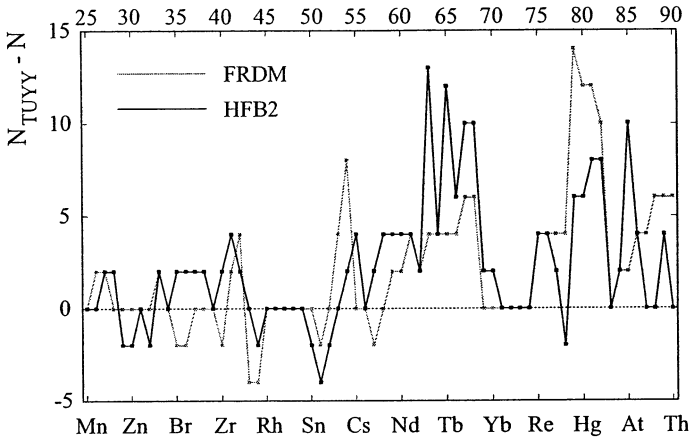

Figure 25. Difference of the calculated location of the r-process (assuming a path along S_n = 3 MeV) between the mass model of Tachibana, Uno, Yamada, and Yamada (TUYY) ([18]) and the two other mass models indicated in the figure.

for the r-process a description similar to figure 20 instead of figure 21 has to be chosen.

The deviations between the models for the constant Z description was significantly larger than the constant N description. Figure 25 shows the difference between the models for the location along an isotopic chain, where the neutron separation energy drops below 3 MeV for the first time.

The deviations follow closely the trend of the neutron dripline shown in figure 20, however, although still significant, the magnitude of these deviations is not quite as large as for the dripline. This is due to the fact that obviously S_n = 3 MeV is closer to the valley of stability then S_n = 0 MeV, and the divergences of the mass model extrapolations are smaller.

While the neutron dripline may potentially never be reached in the mass region of the r-process, the r-process path has already been explored for nuclei at the $N = 82$ shell and it is anticipated that the major part of the r-process path will be mapped with the next generation radioactive beam facilities. The most important nuclear quantities that have to be measured for nuclei along the r-process are the masses to determine the neutron separation energies and the lifetimes.

7. Future of Dripline Studies

The present day facilities will not be able to push the knowledge of the driplines much further. Increases of primary beam intensities at projectile fragmentation facilities might discover a few more isotopes at the proton dripline below $Z = 50$ and at the neutron dripline for $N < 30$. The possible observation of proton dripline nuclei above $Z = 50$ using projectile fragmentation [228] could be explored further and might compete with fusion evaporation reactions. Improvements of the sensitivity of the fusion evaporation reactions could lead to the observation of a few more new isotopes at the proton dripline above $Z = 50$.

Significant advances have to wait for the next generation radioactive beam

facilities. Many different approaches are currently being pursued, for example the Radioactive Ion Beam Factory at RIKEN [229] and the International Facility at GSI [230] as projectile fragmentation facilities and next generation ISOL type machine EURISOL [231]. The proposal for RIA, the Rare Isotope Accelerator in the U.S. combines the two approaches [232].

These new facilities will be able to produce hundreds of new nuclei, most of them towards the neutron dripline.

7.1. Proton Dripline

It is important to distinguish between observing new nuclei at and beyond the dripline and measuring the dripline itself. As was pointed out earlier, the actual location of the proton dripline is virtually unknown beyond $Z = 12$. In order to determine the proton dripline, high resolution mass measurements of the nuclei at and beyond the dripline are necessary. Recent advances in storage rings [233] and ion traps [234, 235] resulted in many new measured masses during the last few years. Over 300 new masses have been reported since the mass evaluation of 1997 [236] and they are included in the most recent NUBASE evaluation [126]. It is conceivable that the proton dripline for at least the odd-Z nuclei will be mapped experimentally within the next few years.

The observation of new nuclei beyond the dripline and the determination of the actual location of the limit of nuclear existence is probably harder. In the heavy mass region ($Z \sim 80$) nuclei with lifetimes of the order of picoseconds can be located up to ~ 11 neutrons away from the driplines [175].

Figure 26 shows the presently known nuclei (black squares), the dripline calculated by TUYY [18] (dashed line), and a simple extrapolation of the lifetime limit of $\sim 10^{-9}$s

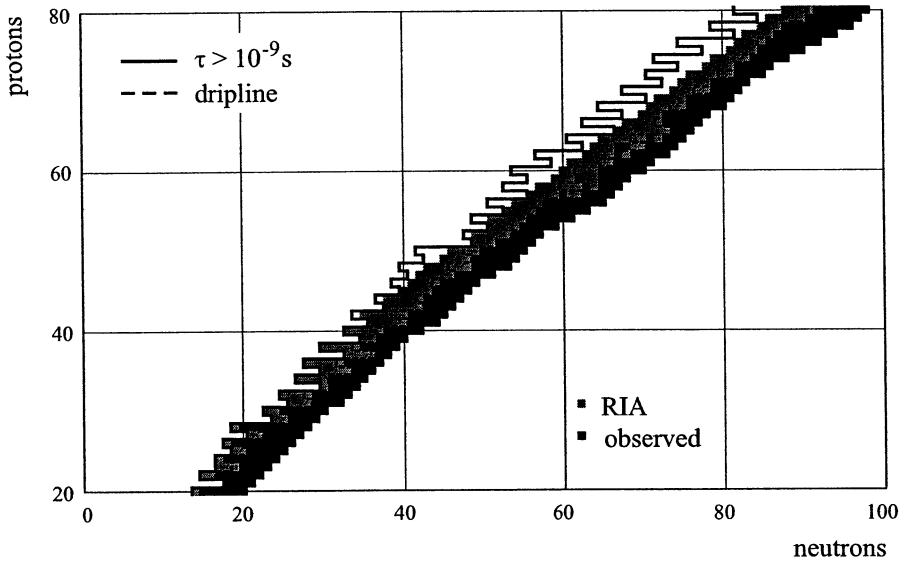

Figure 26. Reach of the proposed rare isotope accelerator RIA at and beyond the proton dripline.

(solid line). The grey squares show the estimated reach of the proposed Rare Isotope Accelerator with a production limit of approximately one nucleus per day. The figure shows that RIA will be able to map out the whole dripline including all even-Z nuclei up to $Z = 80$. RIA has the potential to produce well over 200 new nuclei most of them beyond the proton dripline. About 100 nuclei will still be out of reach.

In addition to the direct production of these nuclei via projectile fragmentation, the high intensities for radioactive nuclei closer to the dripline will potentially make fusion evaporation reactions with these nuclei possible. Thus the limitation of stable projectiles shown in figure 9 is not relevant anymore and new nuclei at and beyond the proton dripline might also be populated with fusion evaporation reactions with radioactive projectiles. The expected reduced beam intensity might be compensated by the choice of evaporation channels with larger cross sections. For nuclei beyond $Z \sim 80$, this might be the only chance to further explore the proton dripline.

7.2. Neutron Dripline

The neutron dripline is significantly harder to reach than the proton dripline. Even RIA will not be able to produce all bound neutron-rich nuclei. Figure 27 shows the presently observed nuclei (black squares), the neutron dripline predicted by TUYY [18] (solid line) and the nuclei expected to be populated at RIA with a rate of one per day (grey squares). It is expected that RIA will reach the dripline (depending on the model) up to $Z \sim 30$ ($N \sim 60$) and the last sighting of the dripline could be at $N \sim 88$.

For the mass region shown in the figure ($Z \leq 50$) approximately 400 new nuclei will be produced with hundreds more above $Z = 50$. However, the neutron dripline itself will be out of reach. Potentially the only chance to advance the knowledge of the neutron dripline even further is secondary fragmentation or secondary fission of radioactive beams. This concept is currently being explored for the next generation European ISOL facility EURISOL [237].

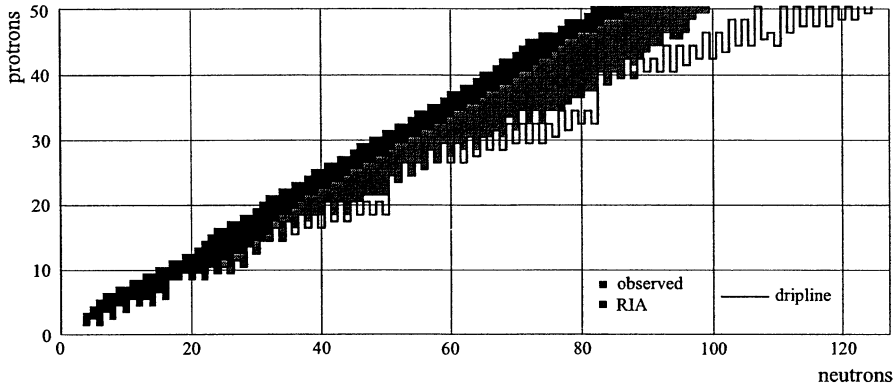

Figure 27. Reach of the proposed rare isotope accelerator RIA at and beyond the neutron dripline.

8. Conclusion

There are at least three different definitions of the driplines. In the present review the dripline was defined as the zero crossing of the neutron or proton separation energies. Others use the typical nuclear timescale of 10^{-22}s as the definition of the dripline, whereas in this review this timescale is referred to as the limit of nuclear existence. A third definition is the condition that the nucleus must be directly observable ($\gtrsim 10^{-9}$s).

The first and the third definition are identical for the neutron dripline. The second definition would include several light mass nuclei with lifetimes of $< 10^{-22}$s. It is not easy to set a sharp limit and the recent charts of nuclei include even nuclei with lifetimes as short as 10^{-22}s.

The location of the proton dripline when defined as $S_p = 0$ is experimentally not well determined. However, this is not critical, because the location of the dripline itself does not have any practical implications. Due to the Coulomb barrier there is no unique experimental signature. Several mass measurements of nuclei in the vicinity of the dripline are necessary in order to locate the $S_p = 0$ dripline. The definition of the dripline related to direct observation is in a sense arbitrary because it will change with time as experimental techniques improve.

No major breakthroughs are expected for the observation of new nuclei at and beyond the dripline in the near future. The improvements of mass measurements should be able to establish the exact location of the proton dripline ($S_p = 0$) for many more nuclei. The neutron dripline might be extended by a few more isotones (or isotopes) with increases in primary beam intensities. In the light mass region neutron and proton coincidence measurements of nuclei beyond the neutron and proton dripline will yield new spectroscopic information. The elusive di-proton emission is finally within experimental reach and additional cases might be found.

However, significant advances will have to wait until the next generation radioactive beam facilities are completed. Overall they will be able to produce more than a thousand of new nuclei. About 200 new nuclei beyond the proton dripline and approximately 400 new nuclei at or very close to the neutron dripline will be accessible.

Acknowledgments

I would like the thank Chasity Fudella for help with the manuscript and Thomas Baumann for the preparation of Figures 2 and 3. I also would like to thank Sam M. Austin, Thomas Baumann, P. Gregers Hansen, and Hendrik Schatz for their comments and suggestions.

References

[1] Nolan P J and Twin P J 1988 *Ann. Rev. Nucl. Part. Sci.* **38** 533
[2] Janssens R V F and Khoo T L 1991 *Ann. Rev. Nucl. Part. Sci.* **41** 32
[3] Moretto L G and Wozniak G J 1993 *Ann. Rev. Nucl. Part. Sci.* **43** 379
[4] Müller B 1995 *Rev. Mod. Phys.* **58** 611
[5] Harris J W and Müller B 1996 *Ann. Rev. Nucl. Part. Sci.* **46** 71
[6] Gutbrod H, Aichelin J and Werner K (editors) 2003 *Proceedings of the 16th International Conference on Ultra-Relativistic Nucleus-Nucleus Collisions* Nucl. Phys. A **715**
[7] Armbruster P 1999 *Rep. Prog. Phys.* **62** 465
[8] Armbruster P 2000 *Ann. Rev. Nucl. Part. Sci.* **50** 411
[9] Hofmann S and Münzenberg G 2000 *Rev. Mod. Phys.* **72** 733

[10] Mueller A C and Sherrill B M 1993 *Ann. Rev. Nucl. Part. Sci.* **43** 529
[11] Jonson B 2004 *Phys. Rep.* **389** 1
[12] Roeckl E 1992 *Rep. Prog. Phys.* **55** 1661
[13] Woods P J and Davids C N 1997 *Ann. Rev. Nucl. Part. Sci.* **47** 541
[14] Livingood J J and Seaborg G T 1940 *Rev. Mod. Phys.* **12** 30
[15] Firestone R B, Shirley V S, Chu S Y F, Baglin C M and Zipkin J 1996 *Table of Isotopes* John Wiley and Sons, New York (1996)
[16] Firestone R B, Chu S Y F and Baglin C M 1998 *1998 Update to the 8th Edition of the Table of Isotopes* John Wiley and Sons, New York (1998)
[17] Firestone R B, Chu S Y F and Baglin C M 1999 *1999 Update to the 8th Edition of the Table of Isotopes* John Wiley and Sons, New York (1999)
[18] Tachibana T, Uno M, Yamada M and Yamada S 1988 *Atomic Data Nucl. Data Tables* **39** 251
[19] Baum E M, Knox H D and Miller T R 2002 *Nuclides and Isotopes - Chart of Nuclides* 16^{th} ed., Knolls Atomic Power Laboratory and Lockheed Martin, Schenectady, New York
[20] Brown B A 1991 *Phys. Rev. C* **43** R1513
[21] Hansen P G and Tostevin J A 2003 *Ann. Rev. Nucl. Part. Sci.* **53** 219
[22] Goldanskii V I 1960 *Ann. Rev. Nucl. Part. Sci.* **16** 1
[23] Cerny J and Hardy J C 1977 *Ann. Rev. Nucl. Part. Sci.* **27** 323
[24] IUPAC Transfermium Working Group 1991 *Pure Appl. Chem.* **63** 879
[25] Antony M S 2002 *Nuclide Chart 2002* Association Européenne contre les Leucodystrophies, Nancy, France
[26] Nefkens B M K 1963 *Phys. Rev. Lett.* **10** 55
[27] Schwarzschild A, Poskanzer A M, Emergy G T and Goldhaber M 1964 *Phys. Rev.* **133** B1
[28] Stevenson J D and Price P B 1981 *Phys. Rev. C* **24** 2102
[29] Langevin M *et al* 1985 *Phys. Lett.* **150B** 71
[30] Artukh A G, Avdeichikov V V, Ero J, Gridnev G F, Mikheev V L, Volkov V V and Wilczynski J 1970 *Phys. Lett.* **33B** 407
[31] Guillemaud-Mueller D *et al* 1990 *Phys. Rev. C* **41** 937
[32] Bowman J D, Poskanzer A M, Korteling R G and Butler G W 1973 *Phys. Rev. Lett.* **31** 614
[33] Sakurai H *et al* 1996 *Phys. Rev. C* **54** R2802
[34] Borrel V *et al* 1992 *Z. Phys. A* **344** 135
[35] Blank B *et al* 1996 *Phys. Rev. Lett.* **77** 2893
[36] Mohar M F *et al* 1991 *Phys. Rev. Lett.* **66** 1571
[37] Blank B *et al* 1995 *Phys. Rev. Lett.* **74** 4611
[38] Dobaczewski J, Hamamoto I, Nazarewicz W and Sheikh J A 1994 *Phys. Rev. Lett.* **72** 981
[39] Dobaczewski J, Nazarewicz W, Werner T R, Berger J F, Chinn C R and Decharge J 1996 *Phys. Rev. C* **53** 2809
[40] Symons T J M *et al* 1979 *Phys. Rev. Lett.* **42** 40
[41] Cerny J, Pehl R H, Goulding F S and Landis D A 1964 *Phys. Rev. Lett.* **13** 726
[42] Robertson R G H, Martin S, Falk W R, Ingham D and Djaloeis A 1974 *Phys. Rev. Lett.* **32** 1207
[43] Jelley N A, Wilcox K H, Weisenmiller R B, Wozniak G J and Cerny J 1974 *Phys. Rev. C* **9** 2067
[44] Kashy E, Benenson W, Mueller D, Nann H and Robinson L 1976 *Phys. Rev. C* **14** 1773
[45] Stokes R H and Young P G 1967 *Phys. Rev. Lett.* **18** 611
[46] McGrath R L, Cerny J and Norbeck E 1967 *Phys. Rev. Lett.* **19** 1442
[47] Cerny J, Mendelson Jr. R A, Wozniak G J, Esterl J E and Hardy J C 1969 *Phys. Rev. Lett.* **22** 612
[48] Macfarlane R D and Siivola A 1965 *Phys. Rev. Lett.* **14** 114
[49] Münzenberg G, Faust W, Hofmann S, Armbruster P, Guttner K and Ewald H 1979 *Nucl. Instrum. Methods* **161** 65
[50] Bruske C, Burkhard K H, Huller W, Kirchner R, Klepper O and Roeckl E 1981 *Nucl. Instrum. Methods* **186** 61
[51] Poskanzer A M, Reeder P L and Dostrovsky I 1965 *Phys. Rev.* **138** B18
[52] Poskanzer A M, Cosper S W and Hyde E K 1966 *Phys. Rev. Lett.* **17** 1271
[53] Poskanzer A M, Butler G W, Hyde E K, Cerny J, Landis D A and Goulding F S 1968 *Phys. Lett.* **27B** 414
[54] Thomas T D, Raisbeck G M and Boerstling P 1968 *Phys. Lett.* **27B** 504
[55] Klapisch R, Philippe C, Suchorzewska J, Detraz C and Bernas R 1968 *Phys. Rev. Lett.* **20** 740
[56] Klapisch R, Philippe C, Detraz C, Chaumont J, Bernas R and Beck E 1969 *Phys. Rev. Lett.* **23** 652

[57] Klapisch R, Thibault C, Poskanzer A M, Prieels R, Rigaud C and Roeckl E 1972 *Phys. Rev. Lett.* **29** 1254
[58] Langevin M, Detraz C, Guillemaud-Mueller D, Mueller A C, Thibault C, Touchard F and Epherre M 1983 *Phys. Lett.* **125B** 116
[59] Hansen P G 1979 *Ann. Rev. Nucl. Part. Sci.* **29** 69
[60] Geissel H, Münzenberg G and Riisager K 1995 *Ann. Rev. Nucl. Part. Sci.* **95** 163
[61] Artukh A G, Gridnev G F, Mikheev V L and Volkov V V 1969 *Nucl. Phys. A* **137** 348
[62] Artukh A G, Avdeichikov V V, Gridnev G F, Mikheev V L, Volkov V V and Wilczynski J 1970 *Phys. Lett.* **31B** 129
[63] Artukh A G, Avdeichikov V V, Chelnokov L P, Gridnev G F, Mikheev V L, Vakatov V I, Volkov V V and Wilczynski J 1970 *Phys. Lett.* **32B** 43
[64] Artukh A G, Avdeichikov V V, Gridnev G F, Mikheev V L, Volkov V V and Wilczynski J 1971 *Nucl. Phys. A* **176** 284
[65] Auger P, Chiang T H, Galin J, Gatty B, Guerreau D, Nolte E, Pouthas J, Tarrago X and Girard J 1979 *Z. Phys. A* **289** 255
[66] Aysto J, Moltz D M, Xu X J, Reiff J E and Cerny J 1985 *Phys. Rev. Lett.* **55** 1384
[67] Morrissey D G and Sherrill B M 1998 *Proc. Royal Soc. A* **356** 1985
[68] Tarasov O B, Bazin D, Lewitowicz M and Sorlin O 2002 *Nucl. Phys. A* **701** 661
[69] Bazin D, Tarasov O B, Lewitowicz M and Sorlin O 2002 *Nucl. Instrum. Methods A* **482** 314
[70] Kryger R A *et al* 1993 *Phys. Rev. C* **47** R2439
[71] Thoennessen M *et al* 1999 *Phys. Rev. C* **59** 111
[72] Thoennessen M, Yokoyama S and Hansen P. G. 2001 *Phys. Rev. C* **63** 014308
[73] Morris C L, Fortune H T, Bland L C, Gilman R, Greene S J, Cottingame W B, Holtkamp D B, Burleson G R and Moore C F 1982 *Phys. Rev. C* **25** 3218
[74] Seth K K, Artuso M, Barlow D, Iversen S, Kaletka M, Nann H, Parker B and Soundranayagam R 1987 *Phys. Rev. Lett.* **58** 1930
[75] Gurov Yu B, Aleshkin D V, Lapushkin S V, Morokhov P V, Panin A V, Pechkurov V A, Poroshin N O, Sandukovsky V G, Tel'kushev M V and Chernyshev B A 2003 *JETP Lett.* **78** 183
[76] Bernas M *et al* 1997 *Phys. Lett. B* **415** 111
[77] Mittig W and Roussel-Chomaz P 2001 *Nucl. Phys. A* **693** 495
[78] Glasmacher T 1998 *Ann. Rev. Nucl. Part. Sci.* **48** 1
[79] Glasmacher T 2001 *Nucl. Phys. A* **693** 90
[80] Oertzen W von and Vitturi A 2001 *Rep. Prog. Phys.* **64** 1247
[81] Catford W N 2002 *Nucl. Phys. A* **701** 1
[82] Leistenschneider A *et al.* 2002 *Phys. Rev. C* **65** 064607
[83] Korsheninnikov A A *et al* 2003 *Phys. Rev. Lett.* **90** 082501
[84] Korsheninnikov A A *et al* 1994 *Phys. Lett. B* **326** 31
[85] Kryger R A, Azhari A, Brown J, Caggiano J, Hellström M, Kelley J H, Sherrill B M, Steiner M and Thoennessen M 1996 *Phys. Rev. C* **53** 1971
[86] Thoennessen M *et al* 2003 *Phys. Rev. C* **68** 044318
[87] Kryger R A *et al* 1995 *Phys. Rev. Lett.* **74** 860
[88] Azhari A *et al* 1998 *Phys. Rev. C* **57** 628
[89] Zerguerras T *et al* 2004 *Eur. Phys. J. A* page in press
[90] Axelson L *et al* 1996 *Phys. Rev. C* **54** R1511
[91] Markenroth K *et al* 1998 *Phys. Rev. C* **62** 034308
[92] Peters W A *et al* 2003 *Phys. Rev. C* **68** 034607
[93] Angulo C *et al* 2003 *Phys. Rev. C* **67** 014308
[94] Cable M D, Honkanen J, Parry R F, Thierens H M, Wouters J M, Zhou Z Y and Cerny J 1982 *Phys. Rev. C* **26** 1778
[95] Saint-Laurent M G *et al* 1987 *Phys. Rev. Lett.* **59** 33
[96] Cable M D, Honkanen J, Parry R F, Zhou S H, Zhou Z Y and Cerny J 1983 *Phys. Lett.* **123B** 25
[97] Langevin M *et al* 1986 *Nucl. Phys. A* **455** 149
[98] Benenson W, Mueller D, Kashy E, Nann H and Robinson L W 1977 *Phys. Rev. C* **15** 1187
[99] Benenson W, Guichard A, Kashy E, Mueller D and Nann H 1976 *Phys. Rev. C* **13** 1479
[100] Lepine-Szily A *et al* 2002 *Phys. Rev. C* **65** 054318
[101] Benenson W, Kashy E, Kong-A-Siou D H, Moalem A and Nann H 1974 *Phys. Rev. C* **9** 2130
[102] KeKelis G J, Zisman M S, Scott D K, Jahn R, Vieira D J, Cerny J and Ajzenberg-Selove F 1978 *Phys. Rev. C* **17** 1929
[103] Benenson W, Kashy E, Ledebuhr A G, Pardo R C, Robertson R G H and Robinson L W 1978

Phys. Rev. C **17** 1939
[104] Frank N, Baumann T, Bazin D, Clement R R, Cooper M W, Heckman P, Peters W A, Stolz A, Thoennessen M and Wallace M S 2003 *Phys. Rev. C* **68** 054309
[105] Audi G, Wapstra A H and Thibault C 2003 *Nucl. Phys. A* **729** 337
[106] Gomez del Campo J *et al* 2001 *Phys. Rev. Lett.* **86** 43
[107] Mohar M F *et al* 1988 *Phys. Rev. C* **38** 737
[108] Detraz C *et al* 1990 *Nucl Phys. A* **519** 529
[109] Pougheon F *et al* 1987 *Z. Phys. A* **327** 17
[110] Blank B *et al* 2000 *Phys. Rev. Lett.* **84** 1116
[111] Giovinazzo J *et al* 2001 *Eur. Phys. J. A* **11** 247
[112] Hotchkis M A C, Reiff J E, Vieira D J, Blonnigen F, Lang T F, Moltz D M, Xu X and Cerny J 1987 *Phys. Rev. C* **35** 315
[113] Batchelder J C, Moltz D M, Ognibene T J, Rowe, M W and Cerny J 1993 *Phys. Rev. C* **47** 2038
[114] Alburger D E 1978 *Phys. Rev. C* **18** 1875
[115] D'Auria J M *et al* 1977 *Phys. Lett.* **66B** 233
[116] Batchelder J C, Moltz D M, Ognibene T J, Rowe M W, Tighe R J and Cerny J 1993 *Phys. Rev. C* **48** 2593
[117] Kienle P *et al* 2001 *Prog. Part. Nucl. Phys.* **46** 73
[118] Yennello S J, Winger J A, Antaya T, Benenson W, Mohar M F, Morrissey D J, Orr N A and Sherrill B M 1992 *Phys. Rev. C* **46** 2620
[119] Janas Z *et al* 1999 *Phys. Rev. Lett.* **82** 295
[120] Rykaczewski K *et al* 1995 *Phys. Rev. C* **52** R2310
[121] Hencheck M *et al* 1994 *Phys. Rev. C* **50** 2219
[122] Elmroth T, Hagberg E, Hansen P G, Hardy J C, Jonson B, Ravn H L and Tidemand-Petersson P 1978 *Nucl. Phys. A* **304** 493
[123] Schneider R *et al* 1994 *Z. Phys. A* **348** 241
[124] Giovinazzo J *et al* 2002 *Phys. Rev. Lett.* **89** 102501
[125] Pfutzner M *et al* 2002 *Eur. Phys. J. A* **14** 279
[126] Audi G, Bersillion O, Blachot J and Wapstra A H 2003 *Nucl. Phys. A* **729** 3
[127] Blank B *et al* 1994 *Phys. Rev. C* **50** 2398
[128] Schardt D, Batsch T, Kirchner R, Klepper O, Kurcewicz W, Roeckl E and Tidemand-Petersson 1981 *Nucl. Phys. A* **368** 153
[129] Page R D, Woods P J, Bennett S J, Freer M, Fulton B R, Cunningham R A, Groves J, Hotchkis M A C and James A N 1991 *Z. Phys. A* **338** 295
[130] Page R D, Woods P J, Cunningham R A, Davinson T, Davis N J, James A N, Livingston K and Sellin P J 1994 *Phys. Rev. Lett.* **72** 1798
[131] Janas Z *et al* 1997 *Nucl Phys. A* **627** 119
[132] Soramel F *et al* 2001 *Phys. Rev. C* **63** 031304
[133] Zhankui L, Shuwei X, Yuanxiang X, Ruichang M, Yuanxiu G, Chunfang W, Wenxue H and Tianmei Z 1997 *Phys. Rev. C* **56** 1157
[134] Bogdanov D D, Bugrov V P and Kadmenskii S G 1990 *Sov. J. Nucl. Phys.* **52** 229
[135] Xu S-W *et al* 1999 *Phys. Rev. C* **60** 061302
[136] Mahmud H *et al* 2002 *Eur. Phys. J. A* **15** 85
[137] Shuwei X *et al* 1996 *Z. Phys. A* **356** 227
[138] Yuanxiang X, Shuwei X, Zhankui L, Yong Y, Qiangyan P, Chunfang W and Tianmei Z 1999 *Eur. Phys. J. A* **6** 239
[139] Rykaczewski K *et al* 1999 *Phys. Rev. C* **60** 011301
[140] Karny M *et al* 2003 *Phys. Rev. Lett.* **90** 012502
[141] Batchelder J C *et al* 1998 *Phys. Rev. C* **57** R1042
[142] Xu S W, Li Z K, Xie YX, Wang X D, Guo B, Leng C G and Yu Y 2001 *Eur. Phys. J. A* **12** 1
[143] Sellin P J, Woods P J, Davinson T, Davis N J, Livingston K, Page R D, Shotter A C, Hofmann S and James A N 1993 *Phys. Rev. C* **47** 1933
[144] Hofmann S, Münzenberg G, Heßberger F, Reisdorf W, Armbruster P and Thuma B 1981 *Z. Phys. A* **299** 281
[145] Uusitalo J *et al* 1999 *Phys. Rev. C* **59** R2975
[146] Page R D *et al* 1992 *Phys. Rev. Lett.* **68** 1287
[147] Hofmann S *et al* 1989 *Z. Phys. A* **333** 107
[148] Bingham C R *et al* 1996 *Phys. Rev. C* **54** R20
[149] Seweryniak D *et al* 1999 *Phys. Rev. C* **60** 031304
[150] Poli G L *et al* 1999 *Phys. Rev. C* **59** R2979

[151] Toth K S, Batchelder J C, Moltz D M and Robertson J D 1996 *Z. Phys. A* **355** 225
[152] Davids C N *et al* 1998 *Phys. Rev. Lett.* **80** 1849
[153] Hofmann S, Reisdorf W, Münzenberg G, Hessberger F P, Schneider J R H and Armbruster P 1982 *Z. Phys. A* **305** 111
[154] Scheidenberger C 2002 *Eur. Phys. J. A* **15** 7
[155] Lunney D, Pearson J M and Thibault C 2003 *Rev. Mod. Phys.* **75** 1021
[156] Andreyev A N *et al* 2003 *Eur. Phys. J. A* **18** 55
[157] Andreyev A N *et al* 1999 *Eur. Phys. J. A* **6** 381
[158] Kettunen H *et al* 2003 *Eur. Phys. J. A* **17** 537
[159] Kettunen H *et al* 2001 *Phys. Rev. C* **63** 044315
[160] Tagaya Y *et al* 1999 *Eur. Phys. J. A* **5** 123
[161] Leino M *et al* 1996 *Z. Phys. A* **355** 157
[162] Eskola K *et al* 1998 *Phys. Rev. C* **57** 417
[163] Ikezoe H, Ikuta T, Hamada S, Nagame Y, Nishinaka I, Tsukada K, Oura Y and Ohtsuki T 1996 *Phys. Rev. C* **54** 2043
[164] Mitsuoka S, Ikezoe H, Ikuta T, Nagame Y, Tsukada K, Nishinaka I, Oura Y and Zhao Y L 1997 *Phys. Rev. C* **55** 1555
[165] Malyshev O N *et al* 2000 *Eur. Phys. J. A* **8** 295
[166] Yeremin A V *et al* 1994 *Nucl. Instrum. Methods* **350** 608
[167] Andreyev A N *et al* 1994 *Z. Phys. A* **347** 225
[168] Morimoto K *et al* 2003 *RIKEN Accel. Prog. Rep.* **36** 89
[169] Cagarda P *et al* 2002 *GSI Scientific Report 2001* page 15
[170] Davids C N *et al* 1996 *Phys. Rev. Lett.* **76** 592
[171] Lalazissis G A, Vretenar D and Ring P 2001 *Nucl. Phys. A* **679** 481
[172] Cole B J 1996 *Phys. Rev. C* **54** 1240
[173] Möller P, Nix J R and Swiatecki W J 1995 *At. Data Nucl. Data Tables* **59** 185
[174] Goriely S, Samyn M, Heenen P H, Pearson J M and Tondeur F 2002 *Phys. Rev. C* **66** 024326
[175] Novikov Yu N *et al* 2002 *Nucl. Phys. A* **697** 92
[176] Grigorenko L V,Johnson R C, Mukha I G, Thompson I J and Zhukov M V 2000 *Phys. Rev. Lett.* **85** 22
[177] Grigorenko and Zhukov M V 2003 *Phys. Rev. C* **68** 054005
[178] Ormand W E 1996 *Phys. Rev. C* **53** 214
[179] Geesaman D F, McGrath R L, Lesser P M S, Urone P P and VerWest B 1977 *Phys. Rev. C* **15** 1835
[180] Bain C R *et al* 1996 *Phys. Lett. B* **373** 35
[181] Fynbo H O U *et al* 2000 *Nucl. Phys. A* **677** 38
[182] Mukha I and Schrieder G 2001 *Nucl. Phys. A* **690** 280c
[183] Hinds S, Middleton R, Litherland A E and Pullen D J 1961 *Phys. Rev. Lett.* **6** 113
[184] Sakurai H *et al* 1999 *Phys. Lett. B* **448** 180
[185] Tarasov O *et al* 1997 *Phys. Lett. B* **409** 64
[186] Poskanzer A M, Esterlund R A and McPherson R 1965 *Phys. Rev. Lett.* **15** 1030
[187] Evseev V S, Kurbatov V S, Sidorov V M, Velyaev V B, Wrzecionko J, Daum M, Frosch R, McCulloch J and Steiner E 1981 *Nucl. Phys. A* **352** 379
[188] Golovkov M S *et al* 2003 *Phys. Lett. B* **566** 70
[189] Meister M *et al* 2002 *Phys. Rev. Lett.* **88** 102501
[190] Young B M *et al* 1994 *Phys. Rev. C* **49** 279
[191] Meister M *et al* 2003 *Phys. Rev. Lett.* **91** 162504
[192] Meister M *et al* 2003 *Nucl. Phys. A* **723** 13
[193] Belozyorov A V, Borcea C, Dlouhy Z, Kalinin A M, Kalpakchieva R, Nguyen H C, Oganessian Yu Ts and Penionzhkevich Yu E 1986 *Nucl. Phys. A* **460** 352
[194] Chen L, Blank B, Brown B A, Chartier M, Galonsky A, Hansen P G and Thoennessen M 2001 *Phys. Lett. B* **505** 21
[195] Talmi I and Unna I 1960 *Phys. Rev. Lett.* **4** 469
[196] Amelin A I *et al* 1990 *Sov. J. Nucl. Phys.* **52** 782
[197] Tanihata I, Hamagaki H, Hashimoto, O, Shida Y, Yoshikawa N, Sugimoto K, Yamakawa O, Kobayashi T and Takahashi N 1985 *Phys. Rev. Lett.* **55** 2676
[198] Simon H *et al* 1999 *Phys. Rev. Lett.* **83** 496
[199] Marques F M *et al* 2002 *Phys. Rev. C* **65** 044006
[200] Guillemaud-Mueller D *et al* 1989 *Z. Phys. A* **332** 189
[201] Baumann T *et al* 2003 *Phys. Rev. C* **67** 061303(R)
[202] Bowman J D, Poskanzer A M, Korteling R G and Butler G W 1974 *Phys. Rev. C* **9** 836

[203] Musser J A and Stevenson J D 1984 *Phys. Rev. Lett.* **53** 2544
[204] Westfall G D *et al* 1979 *Phys. Rev. Lett.* **43** 1859
[205] Poucheon F *et al* 1986 *Europhys. Lett.* **2** 505
[206] Ozawa A *et al* 2003 *Phys. Rev. C* **67** 014610
[207] Meyers W D and Swiatecki W J 1966 *Nucl. Phys. A* **81** 1
[208] Garvey G T 1969 *Ann. Rev. Nucl. Part. Sci.* **19** 433
[209] Fauerbach M, Morrissey D J, Benenson W, Brown B A, Hellstrom M, Kelley J H, Kryger R A, Pfaff R, Powell C F and Sherrill B M 1996 *Phys. Rev. C* **53** 647
[210] Ozawa A, Kobayashi T, Suzuki T, Yoshida K and Tanihata I 2000 *Phys. Rev. Lett.* **84** 5493
[211] Thoennessen M 2003 *Proceedings of the 3rd International Balkan School on Nuclear Physics* Edited by G Lalazissis Publishing & Graphic Arts Co Thessaloniki Greece p 243
[212] Thirolf P *et al* 2000 *Phys. Lett. B* **485** 16
[213] Otsuka T, Fujimoto R, Utsuno Y, Brown B A, Honma M and Mizusaki T 2001 *Phys. Rev. Lett.* **87** 082502
[214] Notani M *et al* 2002 *Phys. Lett. B* **542** 49
[215] Lukyanov S M *et al* 2002 *J. Phys. G* **28** L41
[216] Sarazin F *et al.* 2000 *Phys. Rev. Lett.* **84** 5062
[217] Sakurai H *et al* 1997 *Nucl. Phys. A* **616** 311c
[218] Lewitowicz M *et al* 1990 *Z. Phys. A* **335** 117
[219] Sorlin O *et al.* 1993 *Phys. Rev. C* **47** 2941
[220] Glasmacher T *et al.* 1997 *Phys. Lett. B* **395** 163
[221] Ajdacic V, Cerino M, Lalovic B, Paic G, Slaus I and Tomas P 1965 *Phys. Rev. Lett.* **14** 444
[222] Detraz C, Cerny J and Pehl R H 1965 *Phys. Rev. Lett.* **14** 708
[223] Schatz H *et al* 1998 *Phys. Rep.* **294** 167
[224] Qian Y Z 2003 *Prog. Part. Nucl. Phys.* **50** 153
[225] Meyer B S 1994 *Ann. Rev. Astron. Astrophys.* **32** 153
[226] Käppeler F, Thielemann F K and Wiescher M 1998 *Ann. Rev. Nucl. Part. Sci.* **48** 175
[227] Pfeiffer B, Kratz L, Thielemann F K 1997 *Z. Phys. A* **357** 235
[228] Souliotis G A 2000 *Phys. Scr.* **T88** 153
[229] Motobayashi T 2003 *Nucl. Instr. and Meth. B* **204** 736
[230] Henning W F 2003 *Nucl. Instr. and Meth. B* **204** 725
[231] Vervier J 2003 *Nucl. Instr. and Meth. B* **204** 759
[232] Sherrill B M 2003 *Nucl. Instr. and Meth. B* **204** 765
[233] Geissel H and Wollnik H 2001 *Nucl. Phys. A* **693** 19
[234] Bollen G 2001 *Nucl. Phys. A* **693** 3
[235] Bollen G 2002 *Eur. Phys. J. A* **15** 237
[236] Audi G, Bersillion O, Blachot J and Wapstra A H 1997 *Nucl. Phys. A* **624** 1
[237] Helariutta K, Benlliure J, Ricciardi M V and Schmidt K H 2003 *Eur. Phys. J. A* **17** 181